FTD-HC-23-87-70

FOREIGN TECHNOLOGY DIVISION

SEISMIC EFFECTS AND CRATERING DURING
UNDERGROUND BLASTS
(Selected Articles)

Distribution of this document is unlimited. It may be released to the Clearinghouse, Department of Commerce, for sale to the general public.

FTD-HC-23-87-70

EDITED TRANSLATION

SEISMIC EFFECTS AND CRATERING DURING UNDERGROUND BLASTS
(Selected Articles)

English pages: 62

Source: Nauchno-tekhnicheskoye gornoye obshchestvo. vzryvnoye delo, 1968, No. 64/21, pp. 5-24, 158-191

Translated under contract no.
F33657-70- D-0607-P002

UR/2996-68-000-021

PREPARED BY:

TRANSLATION DIVISION
FOREIGN TECHNOLOGY DIVISION
WP-AFB, OHIO.

TABLE OF CONTENTS

AN INVESTIGATION OF CAVERN DEVELOPMENT IN THE CAMOUFLET EXPLOSION

V.N. Rodionov, I.A. Sizov, and V.M. Tsvetkov

Formation of a blast cavern is particularly distinctive among the various effects of an explosion in a solid medium. Although the formation of the cavern integrates into itself all of the developmental details of the blast process, its volume is most sensitive to the strength of the medium. While the ratio of cavern volume to charge weight (ejection index) amounts to 10^2-10^3 liters/kg of TNT for weak clays and loams, this ratio comes to only a few liters/kg of TNT for hard rock.

The schematization of the blast-development process in a dense solid medium described in [1] can be used to derive an expression for determination of cavern volume as a function of the medium's properties. It considers the explosion of a concentrated charge set deep enough so that the free surface of the medium is not broken. An explosion of this type is called a **camouflet-charge explosion.**

Detonation of the charge converts the chemical energy of the explosive (BB) into the potential energy of compressed gases. A shock wave forms in the medium surrounding the charge under the action of gas pressure and sets the medium in motion. The medium undergoes brittle fracture in the shock-wave front around the center of the blast. The granular medium formed as a result resists shearing deformations in accordance with the Coulomb law of dry friction. Experimental studies of explosions in sand have shown that expenditure of energy to perform work against forces of internal friction is the basic mechanism by which the energy of the blast is dissipated, while energy dissipation at the shock-wave front is of secondary importance [6]. Subsequent amplitude decrease on the shock-wave front has as a consequence that

the wave no longer causes any noteworthy destruction.

The zone of broken rock continues to expand even after the compression-wave front has begun to move out ahead of the rubble boundary. This is because the annular stresses in the medium become tensile behind the compression-wave front, with the result that a broadening zone of radial cracks forms.

In the final developmental stage of the blast process, when the boundary of the rubbled zone is moving at low velocity, the distribution of stresses and strains in an undisturbed elastic medium can be taken from the static solution [1]. In the zone of destruction, on the other hand, where the medium is assumed incompressible because its motion is slow, its behavior is described by an equation of motion with inertial terms. The solution obtained can be used within certain limits when the destruction-front velocity remains below that of the elastic waves. The solution of A.S. Kompaneyets [2] is used in the initial stage of the motion, when the compression-wave front is simultaneously the destruction front. The solutions for the initial and final stages are spliced at the instant when the stress in the compression-shock wave equals the ultimate compressive stress of the medium and the wave front begins to lead the destruction front.

Finally, the following expression has been derived [1] for the maximum cavern volume in the case of brittle fracture of the medium as a function of blast energy and the basic properties of the medium (ultimate compressive strength σ^* and compressibility, the latter characterized by the product of density ρ by the square of the velocity of sound V_p):

$$\frac{4}{3}\frac{\pi R_{max}^3 \rho v_p^2}{E} = 38\left(\frac{\rho v_p^2}{250\sigma^*}\right)^{3/4}$$

The radius R_{dr} of the destruction zone is related to the maximum cavern radius R_{max} as follows:

$$\frac{R_{dr}}{R_{max}} = \sqrt[3]{\frac{\rho v_p^2}{4\sigma^*}}.$$

The expansion time of the cavern is

$$t_{max} = \frac{2R_{dr}}{v_p}\left(\frac{\rho v_p^2}{250\sigma^*}\right)^{1/4}$$

These expressions are valid in the following intervals of variation of the medium's properties:

$$10^3 < \frac{\rho c_p^2}{\sigma^*} < 10^5;$$

$$0{,}1 < \frac{\rho c_p^2}{p_0} < 1{,}0,$$

where p_0 is the initial pressure of the explosion products defined in terms of the blast energy E, the charge-chamber volume V_0, and the adiabatic exponent γ of the blast products:

$$p_0 = \frac{(\gamma - 1)E}{V_0}.$$

The analysis submitted here is an extension of earlier analyses for the case in which the medium is deformed plastically.

CAVERN FORMATION IN PLASTIC MEDIA

In contrast to brittle rock, where the medium contiguous with the blast center undergoes substantial changes (these are the rubbling and cracking zones), media such as metals and soils, which are said to be plastic, deform without any distinct macroscopic continuity disturbances, although microstructural changes do, of course, take place in them. Usually, the cohesiveness of plastic media is no lower after termination of the deformation process, and sometimes it is even higher. This is the basis, for example of the work-hardening of metals, which is accomplished by deforming them plastically. However, to avoid complicating the scheme of the calculation, we shall not take this effect into account. Let us present the behavior of the plastic medium outside the elastic region by the equation of ideal plasticity:

$$\sigma_{\varphi\varphi} - \sigma_{rr} = \tau. \qquad (1)$$

In addition to τ, the medium is characterized by a density ρ, a speed of sound v_p, and a Poisson's ratio ν. We shall consistently assume that the medium is not irreversibly compacted.

In its general features, the computation scheme is the same as that for brittle fracture [1]. Arguments common to the two cases will therefore be omitted.

Final stage in cavern development. At the instant when the motion stops, the medium around the cavern has been divided into two zones – plastic and elastic.

In the elastic zone, the stresses σ_{rr}, $\sigma_{\varphi\varphi}$ and strains u_{rr}, $u_{\varphi\varphi}$ of the medium are described by the expressions [3]

$$\left.\begin{aligned} \sigma_{rr} &= -\frac{2}{3}\tau\left(\frac{R_{pl}}{r}\right)^3; \quad u_{rr} = -\frac{2}{3}\cdot\frac{1-\nu}{1-2\nu}\cdot\frac{\tau}{\rho c_p^2}\left(\frac{R_{pl}}{r}\right)^3; \\ \sigma_{\varphi\varphi} &= \frac{1}{3}\tau\left(\frac{R_{pl}}{r}\right)^3; \quad u_{\varphi\varphi} = \frac{1}{3}\cdot\frac{1-\nu}{1-2\nu}\cdot\frac{\tau}{\rho c_p^2}\left(\frac{R_{pl}}{r}\right)^3. \end{aligned}\right\} \qquad (2)$$

The boundary between the elastic and plastic zones has a displacement $r = R_{pl}$:

$$\delta(R_{pl}) = \int_{R_{pl}}^{\infty} |u_{rr}|dr = \frac{1}{3}\cdot\frac{1-\nu}{1-2\nu}\cdot\frac{\tau}{\rho c_p^2} R_{pl}.$$

In the plastic region, the state of the medium at standstill is described by the equilibrium equation

$$\frac{d\sigma_{rr}}{dr} + \frac{2(\sigma_{rr}-\sigma_{\varphi\varphi})}{r} = 0.$$

Taking $r = R_{pl}$ as the plastic boundary

$$\sigma_{\varphi\varphi} - \sigma_{rr} = \tau,$$

we obtain the solution

$$\sigma_{rr} = 2\tau\left(-\frac{1}{3} + \ln\frac{r}{R_{pl}}\right). \qquad (3)$$

The cavern volume is formed at the expense of the volume of displaced medium at the elastic boundary and bulk deformation in the plasticity zone, i.e.,

$$\frac{4}{3}\pi R^3 = 4\pi R_{pl}^2\delta(R_{pl}) + \int_R^{R_{pl}} 4\pi r^2|\varepsilon(r)|dr.$$

We determine the bulk deformation ε from the expression

$$\varepsilon = \frac{\sigma_{rr} + 2\sigma_{\varphi\varphi}}{3k},$$

where $k = \frac{1+\nu}{1-\nu}\cdot\frac{\rho c_p^2}{3}$ is the coefficient of isostatic compression.

Thus we obtain a relation linking the cavern radius R and the radius R_{pl} of the boundary between the elastic and plastic deformation zones:

$$\frac{R_{pl}}{R} = \sqrt[3]{\frac{(1-2\nu)(1+\nu)}{3(1-\nu)^2}\cdot\frac{\rho c_p^2}{\tau}}. \qquad (4)$$

It is easily shown that, as in the case of brittle fracture, the largest part of the kinetic energy is found in the plasticity zone at times preceding standstill. We shall therefore describe the state of the medium in the elastic region with the equations of static

equilibrium [2]. In the plasticity re ion, we shall regard the medium as incompressible and satisfying the equation of motion

$$\rho_0\left(\frac{\partial u}{\partial t}+u\frac{\partial u}{\partial r}\right)=\frac{\partial \sigma_{rr}}{\partial r}+\frac{2(\sigma_{rr}-\sigma_{\varphi\varphi})}{r}. \tag{5}$$

The incompressibility condition takes the form

$$ur^2=U_{pol}R^2=\lambda(t),$$

where $\lambda(t)$ is an arbitrary function of time and R and U_{pol} are the radius and velocity of the cavern.

Solving the equations of motion with the plasticity condition, we obtain

$$\sigma_{rr}=2\tau\ln r+\frac{\rho_0}{r}\left(\frac{R^2}{2}\cdot\frac{dU_{pol}^2}{dR}+2RU_{pol}^2\right)+\frac{\rho_0}{2}U_{pol}^2\left(\frac{R}{r}\right)^4+C(t) \tag{6}$$

where C(t) is a constant of integration.

The boundary conditions at the cavern and at the plastic boundary take the forms

$$\sigma_{rr}=-p(R)\ \text{for}\ r=R;$$
$$\sigma_{rr}=-\frac{2}{3}\tau\ \text{for}\ r=R_{pl}.$$

Substituting boundary conditions into Expression (6), we eliminate C(t) and obtain the equation of motion for the cavern:

$$\frac{dU_{pol}^2}{dy}+\alpha U_{pol}^2=\frac{\beta}{\rho_0}[p(R)-k\tau], \tag{7}$$

where

$$\alpha=\frac{3-4\frac{R}{R_{pl}}}{1-\frac{R}{R_{pl}}};\quad \beta=\frac{2}{1-\frac{R}{R_{pl}}};$$
$$k=2\left(\frac{1}{3}+\ln\frac{R_{pl}}{R}\right);\quad y=\ln R.$$

Let the pressure in the cavern change adiabatically:

$$p=p_0\left(\frac{R_0}{R}\right)^{3\gamma}, \tag{8}$$

we then obtain the solution of (7) in the form

$$U_{pol}^2=\frac{C_1}{R^\alpha}+\frac{\beta}{\alpha-3\gamma}\cdot\frac{p_0}{\rho_0}\left(\frac{R_0}{R}\right)^{3\gamma}-\frac{\beta}{\alpha\rho_0}k\tau. \tag{9}$$

Assuming that $R = R_n$ and $U_{pol} = U_n$ at a certain initial point in

time, we exclude the integration constant C_1:

$$U_{пол}^2 = \left(\frac{R_н}{R}\right)^3 \left[U_н^2 - \frac{3}{3\gamma - \alpha} \cdot \frac{p_0}{\rho_0} \left(\frac{R_0}{R_н}\right)^{3\gamma} + \frac{3}{\alpha\rho_0} k\tau\right] + \\ + \frac{3}{3\gamma - \alpha} \cdot \frac{p_0}{\rho_0} \left(\frac{R_0}{R}\right)^{3\gamma} - \frac{\beta}{\alpha\rho_0} k\tau. \quad (10)$$

Assuming that $U_{pol} = 0$, we obtain an equation for determination of maximum cavern volume:

$$\left(\frac{R_{max}}{R_н}\right)^3 = 1 + \frac{2\rho_0}{\beta k\tau} U_н^2 - \frac{\alpha}{\alpha - 3\gamma} \cdot \frac{p_0}{k\tau} \left(\frac{R_0}{R_н}\right)^{3\gamma} \times \\ \times \left[1 - \left(\frac{R_н}{R_{max}}\right)^{3\gamma - \alpha}\right]. \quad (11)$$

Thus, to determine maximum cavern volume, it is necessary to know the velocity of the cavern's motion or the kinetic energy of the medium at a certain initial time.

We cannot take quantities as close as we please to the real initial parameters of cavern development as the initial parameters U_n and R_n. When the velocity of the elastoplastic boundary becomes commensurate with that of sound, the equations of static equilibrium will no longer be applicable, with the result that the computation scheme will also become strongly unrealistic.

It will therefore be more advantageous to take as the initial parameters U_n and R_n the radius and velocity of the cavern at the time at which the compression wave ceases to plasticize the medium, i.e., when the plasticity front begins to lag behind the compression-wave front.

Initial stage of cavern development. At this stage, the compression-wave front is simultaneously the front of the plastic wave. The average compacting of the medium in the region enclosed in the compression wave can be characterized thus:

$$\frac{\Delta\rho}{\rho_0} \approx \frac{\sigma}{\rho D_0^2}.$$

If we exclude the zone nearest to the charge, where σ_{rr} and $\sigma_{\phi\phi}$ >> >> τ and the medium behaves as a liquid, it can be assumed that the maximum stress varies in the range

$$\tau < \sigma_{max} < 10\tau.$$

The plastic limit τ is $\tau \approx (10^{-2}$ to $10^{-3})\rho v_p^2$. Hence we obtain the average compacting of the medium as $\Delta\rho/\rho_0 \approx 10^{-2}$.

The kinetic energy of the medium, expressed in terms of cavern radius, takes the form

$$E_{кин} = 4\pi\rho \int_R^{R_\Phi} \frac{u^2}{2} r^2 dr = 2\pi U_{пол}^2 R^3 \left(1 - \frac{R}{R_\Phi}\right). \tag{12}$$

For moderate compacting, $\Delta\rho/\rho_0 \approx 10^{-2}$, the ratio $\frac{R}{R_\Phi}\left(\frac{\Delta\rho}{\rho_0}\right)^{1/3} = 0{,}215$, so that it is sufficient to know the position of the wave front only approximately to calculate the kinetic energy of the medium.

We shall use the solution of A.S. Kompaneyets [2] to evaluate the kinetic energy of the medium; here it is assumed that the compacting on the wave front is constant and independent of wave amplitude, and that the medium behind the front is incompressible.

The equation of motion is the same in this case as for the final stage. We shall therefore write the first integral (6) at once, expressing $\lambda(t)$ in terms of the cavern parameters R and U_{pol}:

$$\sigma_{rr} = 2\tau \ln r + \frac{\rho}{r}\left[\frac{R^2}{2}\cdot\frac{dU_{пол}^2}{dR} + 2RU_{пол}^2\right] + \frac{\rho}{2}U_{пол}^2\left(\frac{R}{r}\right)^4 + C(t).$$

Since $\rho = \rho_0(1 + \varepsilon)$, where $\varepsilon \approx 10^{-2}$, we shall assume $\rho = \rho_0$.

The boundary conditions at the cavern and on the wave front take the form

$$\sigma_{rr} = -p(R);$$
$$\sigma_{rr} = -\rho_0 u_\Phi \frac{dR_\Phi}{dt} = -\rho_0 \varepsilon \left(\frac{dR_\Phi}{dt}\right)^2.$$

These conditions, together with the relationships $\left(\frac{R}{R_\Phi}\right)^3 = \varepsilon$ and $\varepsilon = \frac{u_\Phi}{\frac{dR_\Phi}{dt}}$ can be used to derive the equation of motion of the cavern:

$$\frac{dU_{пол}^2}{dy} + \alpha_1 U_{пол}^2 = \frac{\beta_1}{\rho_0}(p - k_1\tau), \tag{13}$$

where

$$\alpha_1 = \frac{3 - 2\varepsilon^{1/3} + \varepsilon^{4/3}}{1 - \varepsilon^{1/3}}; \quad \beta = \frac{2}{1 - \varepsilon^{1/3}};$$
$$k_1 = \frac{2}{3}\ln\frac{1}{\varepsilon}; \quad y = \ln R.$$

By integrating (13), we obtain the expression

$$U_{пол}^2 = \frac{A}{R^{\alpha_1}} + \frac{\beta_1}{\alpha_1 - 3\gamma} \cdot \frac{p_0}{\rho_0} \left(\frac{R_0}{R}\right)^{3\gamma} - \frac{\beta_1 k_1}{\alpha_1} \cdot \frac{\tau}{\rho_0}. \tag{14}$$

In determining the constant of integration A, we consider that the plastic-deformation mechanism goes into action when the stresses $\sigma_{\phi\phi}$ and σ_{rr} do not greatly exceed the plastic limit τ. Before this, the stresses in the medium are substantially greater than the plastic limit, and their difference is substantially smaller than either of the stresses. Hence we can neglect the second term in the right member of the equation of motion. In this case, the motion of the medium will be described by the equation of motion of an ideal fluid.

With stresses in the medium that are substantially larger than the plastic limit, all of the work done by the blast products will be converted into reversible bulk-deformation energy and kinetic energy of the medium. Thus both energies can be utilized subsequently; for simplicity, we shall assume that all of the work of the blast products goes into kinetic energy of the medium at cavern pressures much in excess of the plastic limit. The mechanism of energy loss by plastic deformation will go into action at a certain cavern pressure $P_{pol} > \tau$.

Let us equate the kinetic energy of the medium to the work done by the blast products in expansion to pressure P_{pol}:

$$2\pi\rho_0 U_{пол}^2 R^3 (1+\varepsilon)(1-\varepsilon^{1/3}) = E\left[1 - \left(\frac{p_{пол}}{p_0}\right)^{\frac{\gamma-1}{\gamma}}\right]. \tag{15}$$

We shall assume, as before, that the cavern pressure varies adiabatically:

$$p = p_0 \left(\frac{R_0}{R}\right)^{3\gamma}.$$

Then, applying these relationships, we can determine the constant of integration A. A numerical check showed that as p_{pol}/τ varies from 10 to 100, the constant A is independent of P_{pol} and equals

$$A = 5\frac{p_0}{\rho_0} R_0^{\alpha_1}.$$

It is necessary to splice the solutions for the final and initial stages of cavern development at the time at which the compression wave begins to lead the front of the plastic wave. On the wave front, both

the radial and azimuthal stresses are compressive. There is not sufficient time for sphericity of the motion to manifest at the front, so that the relation between the radial and azimuthal stresses is determined by the same relationships as in the two-dimensional case [3]:

$$\sigma_{\varphi\varphi} = \frac{\nu}{1-\nu}\sigma_{rr} \tag{16}$$

Applying the plasticity condition, we find the radial stress at the instant of separation of the compression-wave front from the plasticity front:

$$\sigma_{rr} = -\frac{1-\nu}{1-2\nu}\tau. \tag{17}$$

On the other hand, we have on the compression-wave front

$$\sigma_{rr} = -\rho_0 u_\varphi \frac{dR_\varphi}{dt} = -\rho_0 \frac{u_\varphi^2}{c}.$$

and since

$$u_\varphi^2 = U_{max}^2\left(\frac{R}{R_\varphi}\right)^4 = U_{max}^2 c^{4/3},$$

we obtain

$$\sigma_{rr} = -\rho_0 U_{max}^2 c^{1/3}.$$

Applying the expressions for σ_{rr}, we obtain the velocity of the cavern at separation of the compression wave from the plasticity front:

$$U_n^2 = \frac{1-\nu}{1-2\nu}\cdot\frac{\tau}{\rho_0 c^{1/3}}. \tag{18}$$

Numerical solution of (14), applying the expressions for U_n and A, yields the following relationships for determination of the cavern radius R_n at the time at which $U_{pol} = U_n$:

$$\left(\frac{R_n}{R_0}\right)^3 = \frac{1}{23{,}7}\left(\frac{\rho_0}{\tau}\right)^{1.03} - \text{for } \nu = 0{,}45;$$
$$\left(\frac{R_n}{R_0}\right)^3 = \frac{1}{9{,}7}\left(\frac{\rho_0}{\tau}\right)^{1.03} - \text{for } \nu = \frac{1}{3}. \tag{19}$$

These relationships are valid with the condition that $10^2 < p_0/\tau < 10^5$.

The expressions obtained for R_n and U_n permit numerical solution of (11) for maximum cavern size in the final stage. With the condition $1 < \frac{\rho_0}{\rho v_p^2} < 10$; $10^2 < \frac{\rho v_p^2}{\tau} < 10^4$ this solution takes the form

$$\left(\frac{R_{max}}{R_n}\right)^3 = 95\left(\frac{\rho v_p^2}{p_0}\right)^{0.96}\left(\frac{\tau}{\rho v_p^2}\right)^{0.22} - \text{for } \nu = 0{,}45;$$

$$\left(\frac{R_{max}}{R_n}\right)^3 = 15{,}7\left(\frac{\rho v_p^2}{p_0}\right)^{0.94}\left(\frac{\tau}{\rho v_p^2}\right)^{0.17} - \text{for } \nu = \frac{1}{3}. \qquad (20)$$

Eliminating R_n from these relationships, we obtain expressions for determination of maximum cavern volume in terms of the basic parameters ρ, v_p, and τ of the medium:

$$\frac{4}{3}\cdot\frac{\pi R_{max}^3 \rho v_p^2}{E} = 59\left(\frac{\rho v_p^2}{p_0}\right)^{0.03}\left(\frac{\rho v_p^2}{250\tau}\right)^{0.77} - \text{for } \nu = 0{,}45; \qquad (21)$$

$$\frac{4}{3}\cdot\frac{\pi R_{max}^3 \rho v_p^2}{E} = 45\left(\frac{\rho v_p^2}{p_0}\right)^{0.01}\left(\frac{\rho v_p^2}{250\tau}\right)^{0.86} - \text{for } \nu = \frac{1}{3}.$$

The blast energy E is determined by the formula

$$E = \frac{p_0 V_0}{\gamma - 1}.$$

TABLE 1

MEDIUM	DENSITY ρ, g/cm^3	PROPAGATION VELOCITY OF LONGITUDINAL WAVES, v_p, km/s	MODULUS OF COMPRESSION ρv_p^2, kfg/cm^2	PLASTIC LIMIT OF MEDIUM τ, kgf/cm^2	MAXIMUM CAVERN VOL. V_{max}, liters/kg of TNT	
					DATA	
					CALC.	EXP.
Clay	2	1.8	$6.5 \cdot 10^4$	50 - 100	80-140	70-190
Lead	11.3	2.4	$6.5 \cdot 10^5$	150	37	27- 30

The adiabatic exponent γ = 1.25.

The radius of the plastic-deformation zone is related to the maximum cavern radius by

$$R_{pl} = R_{max}\sqrt[3]{\frac{(1-2\nu)(1+\nu)}{3(1-\nu)^2}\cdot\frac{\rho v_p^2}{\tau}}.$$

Numerical integration of the cavern equations of motion in the final stage yields the cavern expansion time t_{pol}:

$$\left.\begin{aligned} t_{pol} &= \frac{1.93R_{m1}}{v_p}\left(\frac{\rho v_p^2}{250}\right)^{1/6} \text{ --for } \nu = 0{,}45; \\ t_{pol} &= \frac{2.2R_{m1}}{v_p}\left(\frac{\rho v_p^2}{250}\right)^{1/6} \text{ --for } \nu = \frac{1}{3}. \end{aligned}\right\} \quad (22)$$

For comparison, Table 1 presents calculated results and test-shot data for lead and clay [5]. For these materials, the plastic deformation mechanism appears to be quite realistic.

The calculated and experimental data agree quite satisfactorily.

CERTAIN EXPERIMENTAL RESULTS FROM STUDY OF BLAST-CAVERN DEVELOPMENT IN BRITTLE MEDIA

The explosion of a concentrated charge in rock forms a cavern whose volume, as was shown in [1, 4], is equal in order of magnitude to the volume displaced outside of the rubble zone, i.e., the volume in the elastic region. Consequently, if the crushed rock did not prevent unloading of the material in the elastic zone, the cavern might contract after the gas pressure in it had dropped. In other words, the potential energy accumulated in the elastic-deformation region may give rise to reverse motion of the medium toward the center of the blast. This effect is similar to the thoroughly investigated oscillation of the gas bubble that forms on an explosion in water. With the object of experimental detection of the difference between the maximum and residual cavern volumes under laboratory conditions, we conducted a series of microcharge explosions in blocks of sodium thiosulfate. Cavern pressure was measured by a specially developed technique; residual volume was also registered in each experiment.

Experimental method and results. The physicomechanical characteristics of the sodium thiosulfate $Na_2S_2O_3 \cdot 5H_2O$ from which the blocks were cast and, for comparison, those of a natural rock (rock salt) are given in Table 2.

The experiments were conducted in a metal case with an internal volume of 300 × 300 × 300 mm^3 and walls 20 mm thick. The sodium thiosulfate, which was first crushed into fragments no larger than 20-30 mm, was fused and the melt cast into the case, one of whose covers was removable. On chilling, the melt formed a homogeneous monolithic block with no internal cavities. The block dimensions were arrived at on the

TABLE 2

ROCK	DENSITY ρ, g/cm^3	GRAIN SIZE mm	WAVE PROPAGATION VELOCITY		POISSON'S RATIO ν	ULTIMATE CRUSHING STRENGTH σ^*, kgf/cm^2	MELTING POINT T_{pl}, DEGREES
			LONGITUDINAL WAVES, v_p, km/s	TRANSVERSE WAVES, v_s, km/s			
Sodium Thiosulfate	1.7	<1	4.0	2.2	0.282	200	48
Rock salt	2.15	1-10	4.4	2.4	0.305	400	800

basis of the condition that the cavern have time to reach its maximum size during the time required for the wave to reach the limits of the block. The time for development of the cavern to maximum size is closely similar in order of magnitude to the duration of the positive phase of the compression wave radiated on detonation. The duration of the positive phase did not exceed 20 μs in the experiments. At a velocity v_p = 4 km/s, the wave can cover a distance of 80 mm during this time, or little more than half of the distance from the blast center to the faces of the specimen.

Spherical PETN charges with a density ρ = 1.5 g/cm^3 and weights q from 0.2 to 2.4 g were used in the experiments. The explosive charge was inserted into the center of the block through a cylindrical hole, which was then filled with the melt. A liquid-filled metal tube was pushed in as far as the charge from the other side so that the gas pressure in the cavern could be transmitted to the sensing element of a pressure transmitter. Figure 1 shows a diagram of the transmitter. Under the pressure, the deflection of the transmitter's membrane is converted by a barium zirconate piezoelectric element into an electric signal, which is registered by an electronic oscillograph. Steel membranes 30 mm in diameter and 3 mm thick, working in their elastic range, permitted measurement of pressures up to 300 atm.

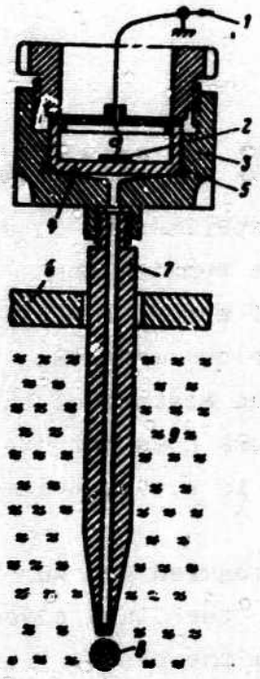

Fig. 1. Pressure transmitter. 1) Lead-out to oscillograph; 2) barium zirconate crystal; 3) transmitter case; 4) membrane; 5) rubber gasket; 6) bomb cover; 7) liquid-filled tube; 8) explosive charge; 9) thiosulfate.

When the pressure p_0 acts on the membrane, an electric charge equal to $e = p_0 S$, where S is the transmitter sensitivity, forms on the plates of the piezoelectric crystal. If C is the total capacitance shunting the transmitter, a voltage $p_0 S/C$ proportional to the pressure to be measured will appear across the crystal's plates. This electrical signal passes through a cathode follower to the input of an OK-24M oscillograph. The registration time was 34 ms in the experiments. The signal was time-swept on photographic film in a rotating drum-type cassette.

The transmitter was calibrated on a special machine to determine its sensitivity. A fixed pressure was applied to the membrane with a hydraulic press and then released. The transmitter signal passed through an amplifier with a cathode follower to the oscillograph input. A square calibration pulse of the reverse polarity and known amplitude was also impressed upon this input. By balancing the signals, it was possible to determine the sensitivity of the transmitter from the known pressure drop, the amplitude of the calibration signal, and the rating of the capacitance shunting the transmitter. The transmitter used in the work has a sensitivity of $260 \cdot 1000$ $mV \cdot nF/kg/cm^2$.

The bore of the tube and the transmitter were filled with liquid after placing the explosive charge. At pressures $p \approx 100$ atm, the liquid in the tube can be regarded as practically incompressible. Blowby of explosion products along the tube outer wall was excluded by pipe-threading it. The tube had no marked effect on the experimental results: the caverns remained spherical and did not differ in volume from caverns produced in control explosions in blocks without the tube.

After an explosion, the block was sectioned along planes passing through the blast cavern, using an saw or an incandescent Nichrome wire.

Fig. 2. Photograph of section through sodium thiosulfate block after explosion of 1-g charge.

Figure 2 presents a qualitative picture of the results of an explosion. The cavern is surrounded by a light-colored zone in which material has been shattered and crushed outward. The boundary of the zone is indistinct, so that its dimensions can be determined only approximately. Next outward is a region of material that has been broken up by brittle cracking. The cracks are preferentially radial in direction and their crossing and branching can be discerned. The cracks are not wide, and it is not evident that they are contaminated by blast products. However, communication between cracks is good, since an attempt to "develop" the shattering zone with a water-etching specimen failed: the water flowed out rapidly along the cracks, all the way to the faces of the block. Several dozen cracks are visible on the section. As charge weight increases, so does the number of cracks, and we observe a trend toward widening of the coarser cracks. A region of unbroken material, which probably belongs to the elastic zone, can be seen outside the zone of radial cracking.

Cavern volume was measured by filling the cavern with modelling clay, and cavern radius was determined as the radius of a sphere of the same volume. In addition to the cavern-volume measurements, the dimensions of the lighter-colored zone were recorded as visually determined in the experiments. This zone was identified with the zone of shattering (in this case, the visual method gives a low-side estimate of shattering-zone dimensions). Figure 3 presents the results of measurement of cavern dimensions and shattering zones for various charges.

The experimental data presented here are in agreement with the principle of geometrical similarity: the radii of the caverns and shattering zones formed are directly proportional to charge dimensions. Thus, $R_p/R_0 = 3$ for the blast caverns and $R_{dr}/R_0 = 9$ for the shattering

zones (R_0, R_p and R_{dr} are the charge, cavern, and shattering-zone radii, respectively). The scatter of the experimental points is ±15%.

As we should expect, the cavern pressure at the instant when maximum size is reached is independent of charge size. Figure 4 shows the form of a typical pressure oscillogram. At first (time a), we see

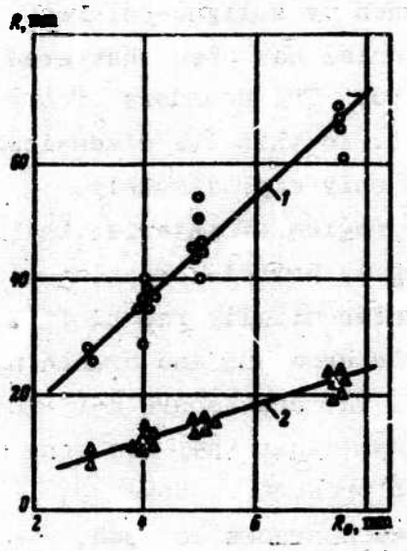

Fig. 3. Curves showing radii of cavern (2) and shattering zone (1) as functions of explosive-charge radius.

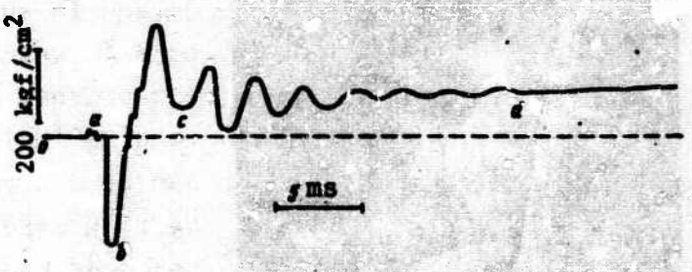

Fig. 4. Oscillogram trace of pressure over time.

the induction corresponding to delivery of the electric pulse to detonate the charge. The first sharp downward jump (time b) is due to arrival of the compression wave propagating through the body of the tube and transmitter; the pressure peak (segment bc) that follows next is due to the action of the shock wave moving through the liquid in the bore. On segment cd, we see rapidly damped oscillations with a period of about 2 ms. The trace then becomes a straight line parallel to the "zero" line, the distance to which is proportional to the gas pressure in the cavern.

We see from comparison of the results from various experiments that oscillogram segment cd is explained by oscillations of the liquid column in the transmitter bore. An estimate indicates that it is sufficient for an air bubble 2-3 mm in diameter to exist in the bore to generate oscillations with a period equal to that observed in the experiments. This effect is quite possible in our experiments. After damping of the oscillations, the pressure-trace curve becomes a straight line whose distance from the "zero" line is proportional to the gas pressure in the cavern. The values of the pressure p as obtained by

reduction of the oscillograms are as follows:

q, g	2.4	2.4	2.4	0.8	0.8	0.4	0.4	0.4
p, atm	110	130	120	120	150	110	115	110

As we see from the experimental data cited, the cavern pressure remains the same, within the limits of error, for explosions of charges of various weights, averaging p = 120 atm. The scatter of the experimental pressure values does not exceed the scatter observed in cavern-volume determination.

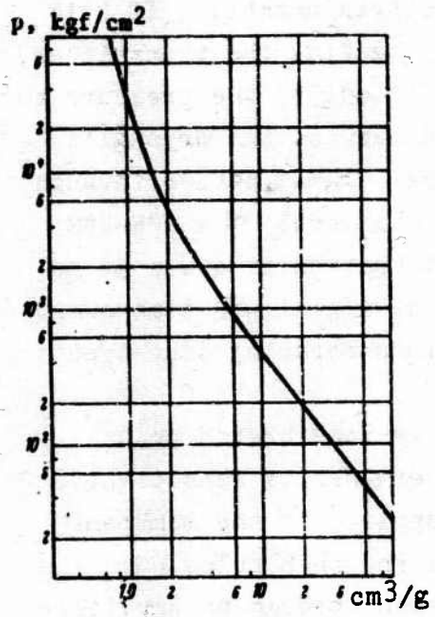

Fig. 5. Adiabatic curve of trimethylenetrinitroamine explosion products.

Let us compare the measured pressure with that corresponding to the final cavern volume found after opening the block. For this purpose, we shall use the adiabatic curve of the blast products. No such curve is available for PETN. The explosion-product adiabatic curve of TNT, which was calculated by Jones [7], is well known, but may lead to substantial errors, since the specific energy Q of TNT is 1 kcal/g, while that of PETN is 1.34 kcal/g. Moreover, the blast products of TNT differ greatly in molecular composition from those of PETN. The blast-product adiabatic curve of trimethylenetrinitroamine, which has been calculated by N.M. Kuznetsov, resembles that of PETN more closely. PETN and trimethylenetrinitroamine yield blast products with a positive oxygen balance and have nearly identical specific energies (at a tamping density $\rho = 1.5$ g/cm^3, trimethylenetrinitroamine has a specific energy of 1.36 kcal/g).

In the explosion of 1 g of PETN, the final cavern volume V_k = = 18 cm^3/g (from the experiment, $R_p/R_0 = 3$). A pressure of 220 kgf/cm^2 corresponds to this specific volume (Fig. 5). This figure is substantially greater than that determined experimentally and cannot be explained by measurement errors. The difference apparently results from measurement of the final cavern volume after the pressure in it has dropped to atmospheric.

Consequently, the result obtained may be regarded as evidence of contraction of the cavern during the drop in its internal pressure.

For a charge weighing 1 g, the largest cavern volume determined through the pressure measurement was $V_{max} = 29$ cm^3/g. Hence $V_k/V_{max} = 0.62$ or $R_k/R_{max} = 0.85$, i.e., the return motion reduces the volume of the blast cavern by about 40%.

TABLE 3

INDICATOR	CHARGE WEIGHTS, g			
	WITHOUT JACKETS	IN MODELLING-CLAY JACKETS		
	0.2, 0.4, 0.8	0.8	0.4	0.2
Ratio of modelling-clay jacket radius (20 mm) to radius of shattering zone	0	0.45	0.55	0.74
Ratio of modelling-clay jacket volume to volume of shattering zone	0	0.09	0.17	0.40
Ratio of final cavern volume to charge volume	27	14	9.4	2.2
Cavern pressure, atm	120	120	100	70
Ratio of maximum cavern volume to charge volume	45	45	51	67

Contraction of the cavern was observed even more distinctly in special experiments in which the charges were detonated in modelling-clay jackets. The shattered rock surrounding a blast cavern exhibits substantial internal friction and cohesion between particles. If some of this rock is replaced by a material whose properties approach those of a liquid, the resistance to the return motion will be reduced and the final cavern volume should differ greatly from the maximum.

In our experiments, the charge was placed at the center of a modelling-clay sphere 40 mm in diameter. With the charge and the pressure-measurement tube, the sphere was set into a block of sodium thiosulfate, so that the pressure corresponding to the maximum cavern

volume arising during cavern development was fixed in the tests.

The results of measurements of the residual cavern volumes, pressures, and maximum cavern volumes, the latter calculated from the measured pressure with the adiabatic curve, appear in Table 3.

The table shows that when charges are detonated in jackets, substitution of modelling clay for 9 to 40% of the rock volume in the shattering zone reduces the maximum cavern volume by no more than a factor of 2 by comparison with unjacketed explosions. However, the volume of the cavern decreases almost to the original volume of the charge when the pressure in it drops to atmospheric.

Strength evaluation of crushed rock. By the time the cavern reaches maximum volume, the material in the shattering zone has been compressed on the cavern side by the expanding gas and at its outer boundary by the normal stress σ^* acting across the cracking zone from the material that has been displaced into the elastic zone. The motion toward the center that follows is governed by unloading of the elastic zone. However, it is decelerated by a certain strength exhibited by the broken medium and by the gas pressure in the cavern. After the pressure has dropped, only the layer of crushed rock impedes the return motion. This circumstance enables us to evaluate the strength of the crushed rock.

If we disregard the cracking zone, it follows from [1] that the cavern radius at time zero will be related to the distance to the elastic zone as follows:

$$\frac{R_{y_0}}{R_{max}} = n = \sqrt[3]{\frac{\rho_0 v_p^2}{4\sigma^*}},$$

where R_{u_0} is the radius of the elastic boundary and R_{max} is the maximum cavern radius.

In spherical coordinates, the equations of motion and continuity for the crushed rock take the form

$$\rho_0\left(\frac{\partial u}{\partial t} + u\frac{\partial u}{\partial r}\right) = \frac{\partial \sigma_{rr}}{\partial r} + \frac{2(\sigma_{rr} - \sigma_{\varphi\varphi})}{r}, \qquad (23)$$

$$\operatorname{div}\vec{u} = 0$$

where ρ_0 is the density of the medium (we shall regard it as constant and equal to the density in the elastic zone); $\underline{u}$ is the velocity at

which the medium is displaced, and σ_{rr} and $\sigma_{\phi\phi}$ are the radial and azimuthal normal stresses, respectively.

The medium is stationary at time zero, and during the motion the elastic-zone boundary is acted upon by a compressive stress equal to $\sigma_{rr}(a)$, where $\underline{a}$ is the displacement of the elastic-zone boundary. Since the density of the medium in the shattering zone is regarded as constant, we can express $\underline{a}$ in terms of the present cavern radius. The change in cavern volume as a result of displacement of the elastic-zone boundary

$$\Delta V = \frac{4}{3}\pi R_{max}^3 - \frac{4}{3}\pi R^3 = 4\pi R_{y_0}^2 a,$$

$$a = \frac{1}{3R_{y_0}^2}(R_{max}^3 - R^3).$$

whence

(24)

We see from (24) that the ratio

$$\frac{a}{R_{y_0}} < \frac{R_{max}^3}{3R_{y_0}^3} = \frac{1}{3n^3} \ll 1,$$

throughout the motion, i.e., we can assume that R_u = const = R_{u_0}.

The relation between the radial and azimuthal normal stresses is written

$$\sigma_{rr} - \sigma_{\varphi\varphi} = k + m(\sigma_{rr} + 2\sigma_{\varphi\varphi}). \qquad (25)$$

The crushed rock is a granular, sandy medium in which m ≈ -1/5. In view of this, Expression (25) can be written

$$\sigma_{\varphi\varphi} = 2\sigma_{rr} - \frac{5}{3}k.$$

The quantity $\underline{k}$ characterizes a certain effective strength of the shattered medium.

It follows from the equation $\vec{u} = \frac{\partial u}{\partial r} + \frac{u}{r} = 0$ for the spherically symmetrical case that

$$u = \frac{\lambda(t)}{r^2},$$

where λ(t) is an arbitrary time function.

Substituting expressions $u = \frac{\lambda(t)}{r^2}$, $\sigma_{\varphi\varphi} = 2\sigma_{rr} - \frac{5}{3}k$ into (23), we obtain

$$\frac{\partial \sigma_{rr}}{\partial r} - \frac{2\sigma_{rr}}{r} + \frac{10}{3} \cdot \frac{k}{r} = \rho_0 \left[\frac{\lambda'(t)}{r^2} - \frac{2\lambda^2(t)}{r^5} \right].$$

Integration over r yields

$$\frac{\sigma_{rr}}{r^2} = \frac{5}{3} \cdot \frac{k}{r^2} + \rho_0 \left[-\frac{\lambda'(t)}{3r^3} + \frac{2\lambda^2(t)}{6r^6} \right] + C(t),$$

where C(t) is another arbitrary time function.

Multiplying both members of this expression by r^2, we obtain

$$\sigma_{rr} = \frac{5}{3} k + \rho_0 \left[-\frac{\lambda'(t)}{3r} + \frac{\lambda^2(t)}{3r^4} \right] + r^2 C(t). \tag{26}$$

We apply the condition at the cavern boundary

$$\sigma_{rr}|_{r=R} = 0.$$

At the boundary of the elastic zone, the radial stresses

$$\sigma_{rr}|_{r=R_y} = -\sigma_{rr}(a).$$

We express the quantities $\lambda(t)$ and $\lambda'(t)$ in terms of the motion parameters at the cavern:

$$\lambda(t) = UR^2; \quad \lambda'(t) = \frac{R^2}{2} \cdot \frac{dU^2}{dR} + 2RU^2.$$

Substituting the boundary conditions and the expressions for $\lambda(t)$ and $\lambda'(t)$ intc (26), we can eliminate the arbitrary time function C(t). We then obtain the equation for the velocity of cavern contraction:

$$\frac{R}{2} \cdot \frac{dU^2}{dR} + U^2 = \frac{3}{\rho_0} \left[\frac{5}{3} k - \left(\frac{R}{R_{y_0}} \right)^2 \sigma_{rr}(a) \right]. \tag{27}$$

In deriving this equation, the quantity $1/n^3$ could be disregarded because of its smallness.

Elasticity theory gives the relation $\sigma_{rr}(a)$:

$$\sigma_{rr}(a) = \sigma^* - \frac{1-2\nu}{1-\nu} \frac{2\rho_0 v_p^2}{R_{y_0}} a, \tag{28}$$

where ν is Poisson's ratio.

Applying Expressions (24) and (28) and introducing the new variable $\bar{R} = R/R_{max}$, we can write (27) in the final form

$$\frac{\bar{R}}{2}\cdot\frac{dU^2}{d\bar{R}}+U^2=\frac{3}{\rho_0}\left\{\frac{5}{3}k-\frac{\bar{R}^3}{n^3}\left[\sigma^0-\frac{1-2\nu}{1-\nu}\cdot\frac{2\rho_0 v_p^2}{3n^3}(1-\bar{R}^3)\right]\right\}.$$

After integrating it, we have

$$U^2=\frac{6v_p^2}{21\bar{R}^2n^3}\left[\frac{35}{2}k\frac{n^3}{\rho_0 v_p^2}\bar{R}^2+\frac{21}{4}\left(\frac{1-2\nu}{1-\nu}\cdot\frac{2}{3}-\right.\right.$$
$$\left.\left.-\frac{\sigma^0}{\rho_0 v_p^2}n^3\right)\bar{R}^4-\frac{1-2\nu}{1-\nu}2\bar{R}^7+A\right].$$

The integration constant A is determined from the condition that $U = 0$ for $\bar{R} = 1$.

As a result, we have

$$U^2=\frac{6v_p^2}{21\bar{R}^2n^3}\left[\frac{35}{2}k\frac{n^3}{\rho_0 v_p^2}(\bar{R}^2-1)+\frac{21}{4}\left(\frac{1-2\nu}{1-\nu}\cdot\frac{2}{3}-\right.\right.$$
$$\left.\left.-\frac{\sigma^0}{\rho_0 v_p^2}n^3\right)(\bar{R}^4-1)+2\frac{1-2\nu}{1-\nu}(1-\bar{R}^7)\right]. \qquad (29)$$

The value of k for sodium thiosulfate can be determined directly from (29). For this purpose, we use the experimentally determined value $\bar{R}_k = 0.85$, at which the cavern reaches its final volume. We then find that $k = 1.4$ kgf/cm^2. As we should expect, the return motion results from the low strength of the shattered medium.

If we analyze this problem with consideration of back pressure, we find that the cavern will hold its dimensions until the pressure in it drops to a few atmospheres.

References

1. Rodionov, V.N. and V.M. Tsvetkov, Prosteyshaya teoriya vzryva sosredotochennogo zaryada v tverdoy srede (An elementary theory of the explosion of a concentrated charge in a solid medium), Trudy V konferentsii po burovzryvnym rabotam (Transactions of Fifth Conference on Drilling and Blasting), Izd-vo "Nedra", 1967.

2. Kompaneyets, A.S. Udarnyye volny v plasticheskoy uplotnyayushcheysya srede (Shock waves in a plastic compacting medium), DAN SSSR, Vol. 109, No. 1, 1956.

3. Landau, L.D. and Ye.M. Lifshits, Teoriya uprugosti (Elasticity theory), Izd-vo "Nauka", 1965.

4. Rodionov, V.N. K voprosy o povyshenii effektivnosti vzryva v tverdoy srede (Improving the effectiveness of an explosion in a solid

medium). Izd. IGD (Institute of Mining) im. A.A. Skochinskogo, 1962.

5. Spravochnik po burovzryvnym rabotam na stroitel'stve (Handbook of construction drilling and blasting operations), Izd-vo literatury po stroitel'stvu, arkhitekture i stroitel'nym materialam, 1962.

6. Romashov, A.N., V.N. Rodionov, and A.P. Sukhotin. Vzryv v uplotnyayushcheysya neogranichennoy srede (Explosion in an infinite compactible medium), DAN SSSR, Vol. 123, No. 4, 1958.

7. Koul.R. Podvodnyye vzryvy (Underwater explosions), Izd-vo "Inostrannaya literatura", 1950.

Symbol List

Manuscript page	Symbol		English equivalent
2	др	dr	shattering, crushing
2	пол	pol	cavern
4	пл	pl	plastic
5	н	n	initial
7	кин	kin	kinetic
7	ф	f	front
12	пл	pl	melting
14	п	p	cavern
16	к	k	final
18	у	u	elastic

ON THE NATURE OF CERTAIN GROUND WAVES EXCITED BY AN UNDERGROUND EXPLOSION

A.N. Romashov

The paper presents results from experimental studies of the ground-motion wave pattern observed in a zone with a radius of several tens of kilometers when charges weighing from 1 to 1000 tons are exploded. An attempt is made to study the motion of the soil in the immediate vicinity of the charge and the process in which seismic (elastic) waves are shaped and radiated over long distances, which has not yet been adequately investigated. A basic shortcoming of research studies in this direction is a certain formalism in reduction and interpretation of the waves on the seismograms. This approach is particularly conspicuous when Rayleigh and Love waves, for whose excitation mechanism a clear physical interpretation appeared only recently, are isolated on the seismograms.

In this paper, we advance the hypothesis that waves excited in explosions and having certain attributes of surface waves may originate in a different manner. Most probably, these waves are excited as a result of heaving of the soil in the epicentral zone. This heaving, a process in which shearing and bulk deformations develop, is a secondary wave source. The comparatively slow progress of this phenomenon[1] is responsible for the low-frequency character of the soil oscillations in the waves radiated.

The article examines questions of the interaction of the various waves with the free surface, investigates the wave patterns observed in different types of soils, and shows that the excitation mechanism and nature of the principal waves are the same for all soils.

The principal objective of the study was to shed light on the wave pattern of the underground blast. Most attention has been devoted to

[1] See page 61 for footnote.

ascertaining the nature of the individual waves and their excitation mechanisms. Quantitative characteristics of the wave parameters are used to the extent that they contribute to solution of the main problem. More complete quantitative data are given in [2, 3, 4] and elsewhere.[2]

The explosion of a charge near the free surface in a comparatively homogeneous rock massif without overlying strata of soft soil is examined in greatest detail. Further, data on explosions in other types of soils are also presented. Where soil types are not indicated, reference is made to an explosion in a homogeneous rock massif.

EXPLOSION IN AN INFINITE MEDIUM

The explosion of a concentrated charge in an infinite medium is simplest to represent, since the soil-motion pattern around the charge exhibits central symmetry. By virtue of the total symmetry of the source, only a single longitudinal wave of the volume type with a spherical frontal divergence is excited by an explosion in an infinite medium. As we know, this divergence gives the strongest damping of the waves with increasing distance; waves with any other divergence (conical or cylindrical) will attenuate more slowly. The basic problem of the investigation for an explosion in an unlimited medium is establishment of the law of damping of the longitudinal wave with distance.

Infinite-massif longitudinal compression wave parameters have now been studied most thoroughly for blasts in loose homogeneous sands with densities of about 1.5-1.6 g/cm^3 [5] and homogeneous rocks of the limestone, marble, and other types [6] with densities of 2.5-2.7 g/cm^3.

An explosion in sand sets up a longitudinal wave in which the deformations near the charge are inelastic in nature. As it propagates, this wave is distended, and the deformations in it become elastoplastic: an elastic wave appears ahead of the plastic-compression-wave front. The propagation velocity of the elastic wave is constant and approximately equal to the speed of sound, while that of the plastic wave is variable. In a zone with a radius ranging up to about five charge radii, the plastic-wave velocity exceeds the speed of sound; then it drops below the speed of sound and diminishes steadily with increasing distance.

Figure 1 shows the typical appearance of the mass-velocity trace for a compression wave in sand. The motion in the compression wave is

[2] See page 61 for footnote.

for the most part limited to displacement of particles away from the blast.

With increasing distance, attenuation of the compression wave's maximum mass velocity in sand takes place, for various blast powers, according to a law [5] expressed by the formula

$$u = 340\left(\frac{q^{1/3}}{r}\right)^{1.8}. \qquad (1)$$

where u is the maximum velocity, cm/s; q is the charge weight, kg; and r is the distance from the center of the charge to the point of measurement, m.

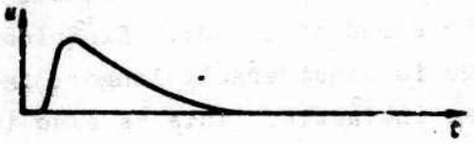

Fig. 1. Typical form of mass-velocity trace of compression wave in sand.

Formula (1) applies in a zone with a radius of 5 to 30 charge radii and characterizes the distance-attenuation law in a plastic compression wave.

The development of an explosion in an infinite rock massif differs somewhat from an explosion in sand. Figure 2 shows the typical form of the mass-velocity trace of a compression wave in a rock massif. To a substantial degree, the propagation of the longitudinal compression wave follows the laws of wave propagation in an elastic medium. Thus, the propagation velocity of the longitudinal compression wave in rocks is practically constant at a value near the speed of sound over the entire range of distances (and even in the immediate vicinity of the charge).

Fig. 2. Typical form of mass-velocity trace of compression wave in rock.

The length of the wave varies very insignificantly with distance. After displacement of the medium away from the blast, we observe a return motion, with the result that particles of the medium are returned to certain positions near their original positions. The ejection index of the blast (the ratio of cavern volume to charge weight) is small, and is measured in the units in many strong rocks. This means that

after the longitudinal compression wave has been radiated, a high excess pressure (about 1000 atm) persists in the blast products. In sandy, clayey, and other types of soils, the ejection index runs into the hundreds, and the residual pressure in the cavern ranges from 10 to 100 atm. This pressure forms a static stress field around the charge, and this field offsets the pressure in the blast products, but for all practical purposes it forms no new waves of appreciable amplitude. The high blast-product pressure in the rocks is explained by the high cohesiveness of these rocks.

If the rock massif behaved as an ideal elastic medium during the explosion, the radiating time of the wave would, as we know, be of the order of magnitude of r_0/v_p (r_0 is the cavern radius or the radius of the explosive (BB) charge, and v_p is the speed of sound). Experience has shown that the actual radiation time is considerably longer, indicating that the medium is to some degree inelastic. This is also indicated by the manner in which the wave damps with distance. The decay of the maximum compression-wave velocity on an explosion in rock follows the same law as on an explosion in sand. In the distance range from 3 to 500 charge radii, this law can be expressed by Formula (1).

The proportionality of velocity to $1/r^{1.8}$ indicates the presence of some absorption of the wave's energy as it propagates even through rock, since attenuation takes place in inverse proportion to distance in a purely elastic medium. The nature of this energy absorption has not yet been established. The exponent 1.8 in Formula (1) characterizes attenuation in a volume wave with spherical divergence. It is valid in a very broad range of distances, extending even to the immediate vicinity of the charge, where inelastic straining takes place, i.e., it characterizes the strongest damping that is possible in the wave. An exception is the zone closest to the charge, extending to a few charge radii, where we observe stronger damping [8]. In subsequent analyses to determine the nature of unknown waves, therefore, it is this exponent of nearly two that we shall use as one of the basic criteria for determining whether a given wave is to be classified as one of the volume type.

Attention should also be drawn to the fact that the parameters of the compression wave in an explosion in an infinite medium vary in accordance with a geometrical law of similarity, i.e., compression-wave

parameters with the dimensions of length and time change in proportion to charge radius on a change in the scale of the explosion.

EXPLOSION NEAR THE FREE SURFACE

An explosion near the free surface is a much more common phenomenon than the explosion in the infinite medium. This is because most blasts that are of practical or scientific interest are detonated under conditions under which the influence of the free surface must be taken into account to one degree or another. This covers all industrial blasting (excavating, rock-crushing, directional and other blasting) and most experimental shots. But even in explosions set off at considerable depth, after which no permanent disturbances of the soil at the epicenter (cracking, heaving, etc.) are observed, and which are still regarded in practice as camouflet explosions, deciphering of the wave pattern still requires consideration of the free-surface effect.

The problem of the blast near a free surface is best broken down into two parts. First, the motion of the soil in the central zone near the charge, i.e., the source generating the waves, is examined, and then the individual waves are described.

Motion of soil in central zone. Before the compression-wave front reaches the free surface, the motion of the soil around the charge follows the same laws as in an explosion in an infinite medium. The influence of the free surface begins to make itself felt only after reflection of the compression wave from this surface, and propagates in the rock in the form of an unloading wave. The propagation velocity of the unloading wave, like that of any other wave, depends on the properties of the medium and has a quite definite value for each type of soil. As a result, the length of time that elapses before the blast products "become aware" of the existence of the free surface is different for different soils.

Arrival of the unloading wave at a given point signifies relief of the compressive stresses at that point and, simultaneously, intensified motion toward the free surface [7]. Thus, by the time the unloading wave reaches the blast cavern, in which a large excess pressure of the gaseous blast products still prevails, much of the soil above the charge will have been unloaded. This means that the blast products can undergo secondary expansion in this direction. The motion of the soil around the charge can be presented schematically as follows. A blast

in an infinite medium is equivalent to enclosing the blast products at high pressure in a spherical container with infinitely thick walls. Bringing the blast closer to the free surface means reducing the thickness of the container walls in a certain direction. Equilibrium of forces can be arrived at in such a system if the material undergoes larger deformations in the direction of the weakened wall than it would with infinitely thick walls. This means that the weakened wall will be buckled outward. The buckling process of the wall is accompanied by corresponding changes in the nature of the deformations. It is obvious that at first, the container wall will deform elastically. If the stresses that arise in it as a result of the elastic strains are inadequate to offset the pressure inside the container, the wall deformations will become plastic. They will increase until the stresses in the material compensate the pressure in the cavern. If the tensile or shearing strength of the material is exceeded during the deformation process, the wall will break and the blast products will erupt through.

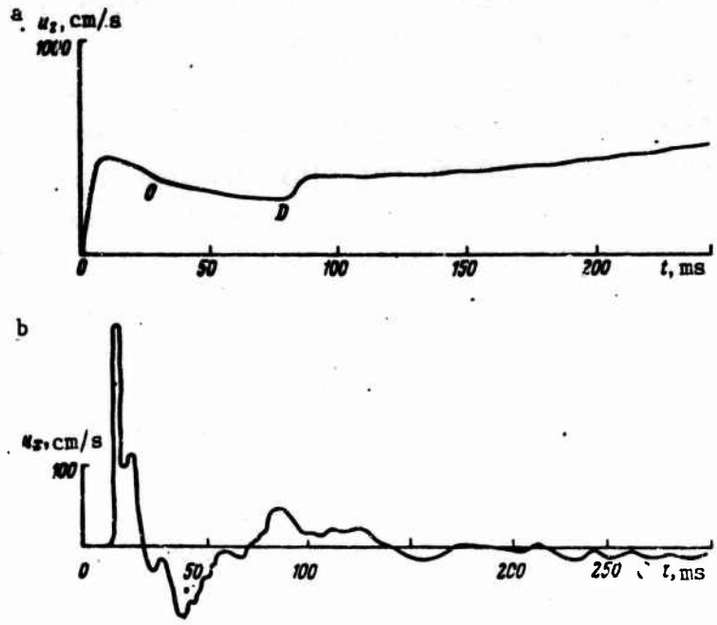

Fig. 3. Mass-velocity oscillograms of ground-surface motion at epicenter (a) and at a point at charge level 75 m from it (b) on explosion of a 150-ton charge at 75-m depth.

A similar heaving process is observed on an explosion in soil near the free surface. As a rule, the free surface is above the charge in such cases. Hence the blast products in the cavern are compensated not only by the stresses in the rock, but also by the weight of the rock above the charge.

The soil motion at the epicenter can be broken down into two phases. The first phase is associated with emergence of the compression wave at the free surface. The second phase, heaving of the ground, corresponds to a quasistatic effect of the blast products that is manifested for the most part in the motion of soil toward the free surface. No soil motion downward or away from the charge is observed during this stage of the explosion's development.

By way of illustration, Fig. 3 shows mass-velocity oscillograms of the motion of the ground surface at the epicenter (a) and at a point located at charge depth 75 m away from it (b) on the explosion of a 150-ton charge buried 75 m deep.

The oscillograms indicate that there is practically no horizontal motion during the second phase, in which the ground rises at the epicenter and whose beginning is marked by the letter D.

The time between emergence of the compression wave at the free surface and the beginning of the second phase is obviously related to the depth at which the charge is set and to the propagation velocities of the compression and unloading waves in the massif. The greater the depth and the slower the waves, the longer will be the time separating the first and second heaving phases. Considering that the wave velocities are different in different soils, we should also expect a substantial difference in the lags of the second phase behind the first. Thus, for example, for an explosion in sand, the secondary soil motion with positive acceleration begins practically simultaneously with the emergence of the compression-wave front at the free surface. Figure 4 presents a mass-velocity oscillogram showing the motion of the epicentral point on an explosion in sand. It also shows a mass-velocity oscillogram for the horizontal motion away from the charge. As in an explosion in rocky soil, no secondary acceleration of the soil in the horizontal direction is observed.

The lack of time separation between the first and second phases for an explosion in sand is obviously due to the facts that the

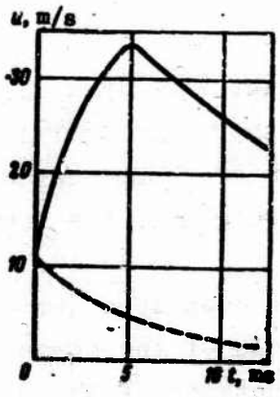

Fig. 4. Mass-velocity oscillograms of ground-surface motion at epicenter (solid line) and at a point situated at charge level 20 cm from it on explosion of a 24-g charge in sand at a depth of 20 cm.

deformation of the sand in the close-in zone is plastic and the unloading propagation velocity nearly infinite.

In explosions in rocky soils, the time segment between the first and second phases is nonzero, since unloading propagates at finite velocity from the free surface. In this connection, it is interesting to make the following observations.

1. Very often, the secondary acceleration of the ground at the free surface begins much later than would follow from the travel time of the wave from the surface to the charge and back.

2. The onset of the second stage in heaving of the ground at the free surface is in most cases accompanied by a rather sharp velocity inflection, indicating instantaneous application of a certain force (see Fig. 3).

These phenomena are obviously related to separation of a certain surface soil layer from the main massif at the epicenter p. This becomes especially conspicuous when the upper layer is a soft soil overlying bedrock (Fig. 5). The inflection marked by the letter D on the mass-velocity oscillograms

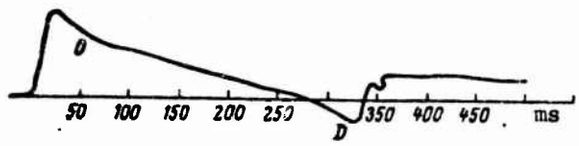

Fig. 5. Mass-velocity oscillogram of ground-surface motion at epicenter on explosion of a charge weighing 10 tons at a depth of 35 m in rocky soil. The top layer of soft soil was 10 m thick.

of ground-surface motion corresponds to rejoining of the layer to the massif, which occurs during the second stage of heaving of the ground above the charge. The slower acceleration of the free surface that

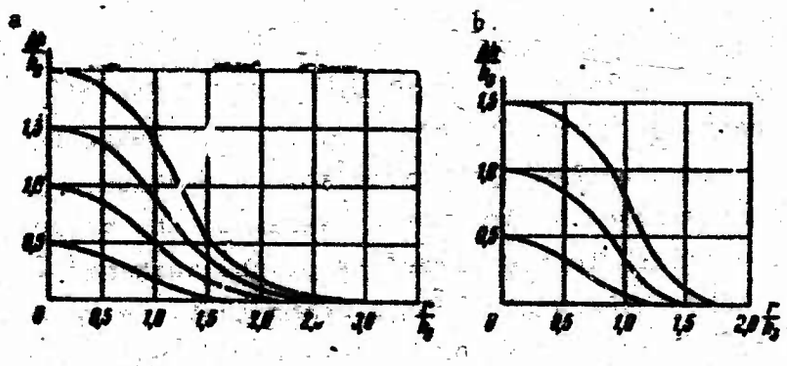

Fig. 6. Shapes of domes formed by underground explosions. a) in dense blue clays; b) in loessy loams; h_z) setting depth of charge; Δh) rise height of dome above ground surface; r) distance from epicenter.

follows corresponds to rising of the layer together with the basic massif.

Figure 6 shows the shapes of the domes observed in blasts in dense clay and loess. The dome is steeper for the explosion in loess, where the cohesion between the soil particles is weaker than it is in clay. It is interesting to note that the shape of the dome in sand is intermediate between the dome shapes for clay and loess, although the cohesiveness of sand is lower. This indicates that dome shape is not determined by cohesive strength alone. Obviously, the heaving of the ground that takes place on peripheral areas in weakly cohesive soils is to a substantial degree simply a consequence of blast-product expansion in the direction of these areas.

Figure 7 shows the shapes of the domes at various times during explosions of 1-ton charges in rocky soil (a) and in clay (b) [5]. We see from Fig. 7 that the heaving of the ground in the form of a smooth dome in the case of the clay blast lasts much longer than in the case of the blast in rocky soil. This difference obviously results from the fact that clay has a large capacity for plastic flow. As a result, the dome retains its shape in clay without breaking up even when the strains in it are no longer elastic. On the other hand, rocky soil breaks up at much smaller strains and, consequently, a dome in rocky soil breaks up earlier.

At the present time, ground motion in the central zone is basically of interest as a source from which waves are radiated. Here, the

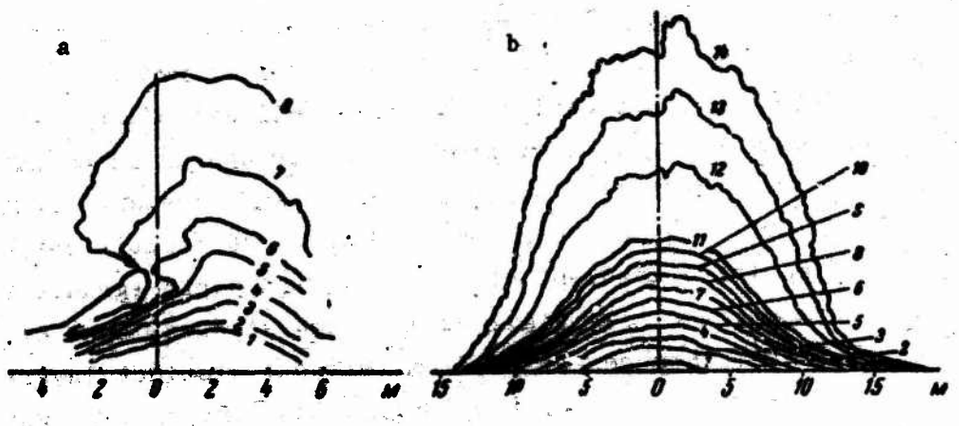

Fig. 7. Shapes of domes at various times during underground explosions of 1-ton charges: a) in rocky soil at 6-m depth; b) in dense blue clays at 7-m depth.

position	1	2	3	4	5	6	7	8	9	10	11	12	13	14
time, ms	0 0	12 20	17 40	25 60	31 80	39 100	44 120	52 140	65 170	— 190	— 210	— 230	— 370	— 440	— 540

greatest interest attaches to stages of the motion in which the soil lifted at the epicenter preserves its bonds with the surrounding massif. It is precisely at these stages that we can expect the most intensive transfer of energy from the central zone into the surrounding massif and, consequently, only the motion in these stages is a wave-radiating source. On the basis of this quite obvious criterion, it will not be difficult to indicate possible differences in the parameters of the waves radiated. Indeed, other conditions the same, the longer the lifted dome retains its bonds to the surrounding soil, the larger will be the energy radiated in the form of waves and the greater will be a certain effective period and the amplitude of the soil motion in these waves. Anticipating somewhat, we can say that the period of the soil vibrations in blast waves in clay is approximately three times longer than for similar blasts in rocky soil; qualitatively, this is fully consistent with the heaving time of the domes in these soils.

Thus, analysis of data from laboratory studies[3] and of the motion of the ground surface in the epicentral zone of the blast indicates that from the standpoint of wave radiation, the explosion near the free

[3]See page 61 for footnote.

surface is a composite radiator that can be resolved as a convention into two independent sources. The first source is the initial stage in development of the blast. In time, this source begins to act when the explosive charge is detonated. Until the compression-wave front reaches the free surface, assuming that the massif is fully homogenecus, we observe a spherically symmetrical pattern of motion of the medium around the charge. Reflection of the compression wave from the free surface results in formation of an unloading wave and a transverse wave that propagates through the massif right behind the compression wave. It is the combination of these waves that forms the wave pattern obtained in solutions of elastic problems in which the blast is represented only as an expansion center. However, a real explosion near a free surface cannot be characterized solely by the longitudinal spherical compression wave. This is because blast products remain in the blast cavern at high excess pressure after the wave has been radiated. This pressure is compensated by the stress field set up in a certain limited zone in the medium around the cavern. And even if the blast takes place in an infinite massif, this stress field persists as long as the pressure is retained in the cavern. The latter drops comparatively slowly, basically as a result of cooling of the gases and gas leakage through the cracks. As a result, the energy of the elastic stresses around the cavern is dissipated slowly without giving rise to waves of appreciable intensity. The situation changes, however, if such a gas-filled cavern is near a free surface. The elastic-strain energy in the rock massif between the cavern the free surface becomes inadequate to offset the gas pressure. The result is buckling of the medium in the direction of the free surface and, consequently, a comparatively rapid pressure drop in the cavern. This, in turn, means that the energy of the elastic stresses in the medium around the cavern will be liberated over a comparatively short time. The dome-shaped heave of the medium in the epicentral zone from blast-product energy and the energy of the elastic stresses in the medium around the cavern is the second source of waves in an explosion near a free surface.

As we see from the mechanism of the second source, it is axially symmetrical and capable of radiating bulk- and shear-strain waves. The preferential motion of the medium in a certain volume around the charge is motion toward the free surface and toward the cavern. Hence it

follows that the second source creates tensile strains. For this reason, the bulk-strain wave radiated by the second source is a decompression wave.

Below we shall examine the strongest waves, which include the longitudinal compression wave radiated during the first expansion stage of the blast products and the transverse and decompression waves excited in the second stage. In addition to these principal waves, other waves may also exist as a result, for example, of interaction between the longitudinal compression wave and the free surface. However, experience has shown that, by comparison with the strong waves cited above, all of the others are of minor significance as regards their amplitudes and the energy that they carry and can be disregarded.

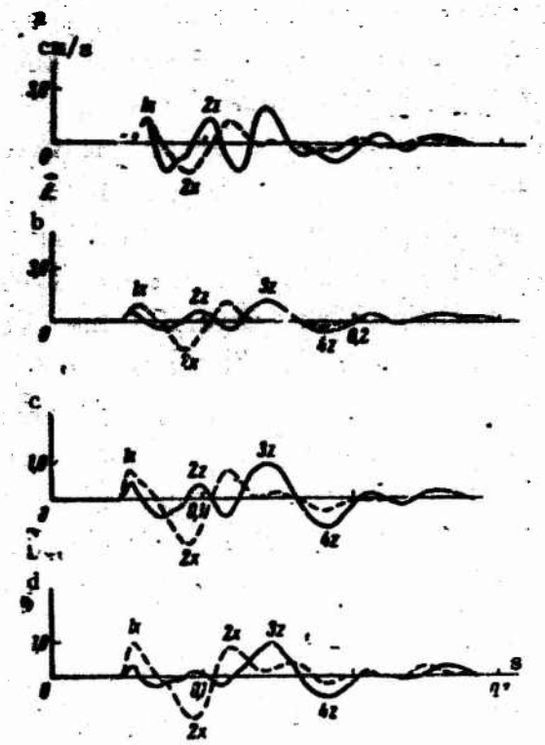

Fig. 8. Mass-velocity oscillograms of the motion of one of the points in the medium at a distance of 245 m from the epicenter on explosion of a 1-ton charge in granite at a depth of 12 m: a) h_p = 0 m; b) h_p = 6 m; c) h_p = 11.4 m; d) h_p = 20 m.

Longitudinal compression wave. This wave is of the same nature as the analogous wave in an explosion in an infinite medium. A property of the longitudinal compression wave in a real explosion near a free surface is that, as a rule, it propagates through an inhomogeneous medium. In most cases, the upper layers of soil present stratified structures. But even in the absence of distinct stratification, there is always a positive gradient of velocity with depth (gradient medium) near the free surface. We shall examine the simplest case of a blast in a comparatively homogeneous medium (without distinct layers near the surface). The interaction of the longitudinal compression wave with the free surface, and the changes in the character and intensity of this wave at various charge and recording-instrument depths, are most conveniently traced in this example.

A typical mass-velocity oscillogram of the motion of the ground in an explosion near a free surface appears in Fig. 8. The first peak on this oscillogram corresponds to the longitudinal compression wave. The low-frequency oscillations observed after passage of the compression wave are caused by other waves and will be considered in detail below.

The propagation velocity of the longitudinal compression wave depends on the properties of the medium. Longitudinal-wave velocity values for certain rocks in which blasts were detonated are given in Table 1.

TABLE 1

ROCK	VELOCITY, m/s		
	LONGITUDINAL WAVE	DECOMPRESSION WAVE	TRANSVERSE WAVE
Loose sand with natural moisture content	150 - 200	—	—
Loessy loam	500 - 600	300 - 330	330
Plastic blue clays	1800 - 2000	750 - 1200	500 - 900
Marbled limestone	6000 - 6200	--	2500 - 2800
Granite	5200 - 5400	4200 - 4500	2000 - 2500

The motion of the medium in the longitudinal compression wave near the free surface is similar in nature to the motion in the compression

wave of an explosion in an infinite massif (see Fig. 2). The maximum velocity of particle motion in the wave is observed a certain time after arrival of the front, i.e., the velocity change in the wave is smooth and not abrupt, as it is in water or in air. After the maximum has been reached, the velocity decreases more slowly to zero, with the positive phase of the compression wave generally several times the velocity rise time to the maximum. After the soil has been displaced away from the explosion, we observe a return motion – the decompression phase. The return motion in the compression wave is about equal in duration to the forward motion and, as a rule, does not exceed it in amplitude.

TABLE 2

meters	cm/s	cm/s		
0	1.4	1.4	120	110
6.0	0.9	0.4	108	37
11.4	0.8	0.5	110	33
20.0	0.9	0.3	150	22

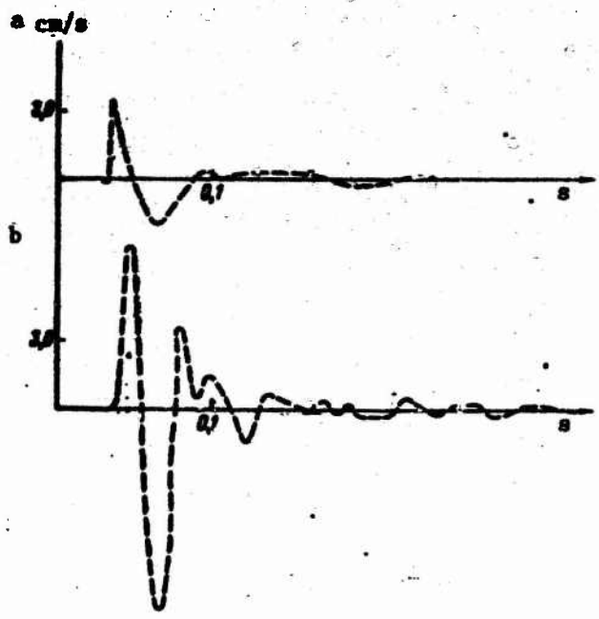

Fig. 9. Mass-velocity oscillograms of soil motion at a distance of 145 m from the epicenter on explosion of a 1-ton charge at 12-meter depth. a) h_p = 15 m; b) h_p = 0 m.

At distances considerably greater than the charge-setting depth, an explosion near the boundary of a homogeneous half-space can be

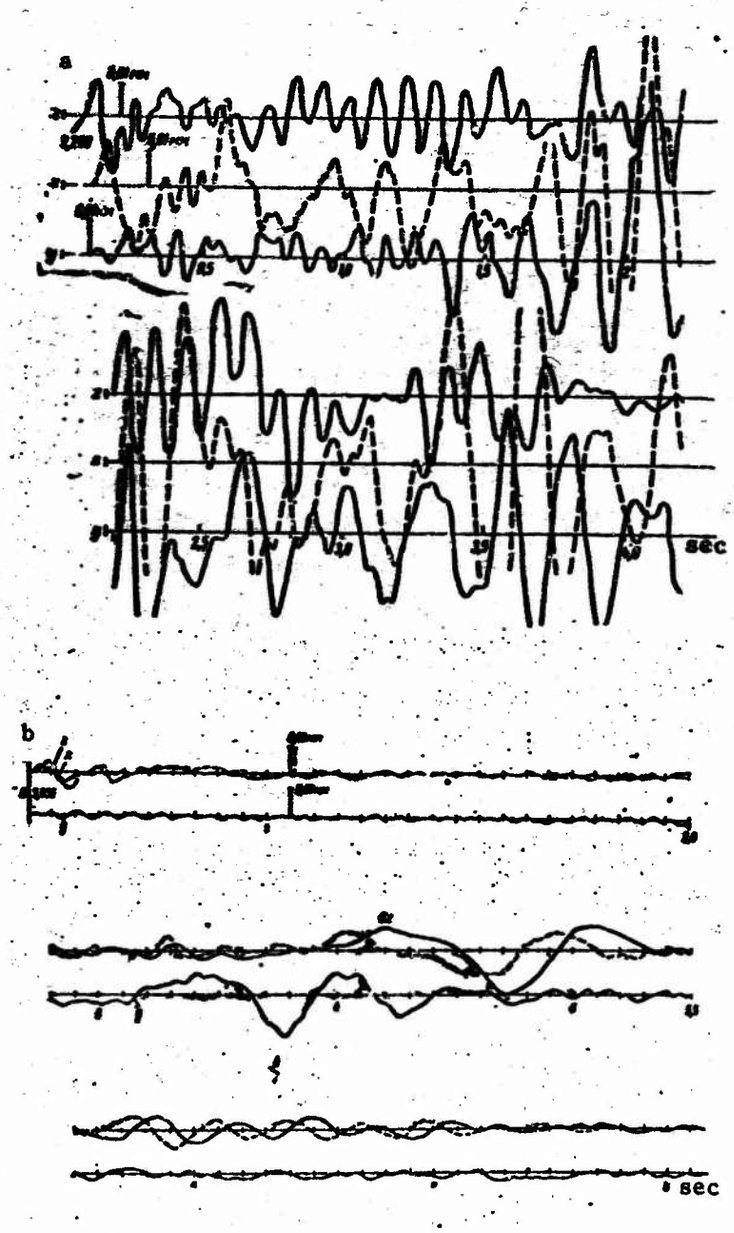

Fig. 10

regarded for practical purposes as a certain source on the free surface that radiates a spherical wave into the half-space. At a certain distance from the blast, the motion in the compression wave on the free

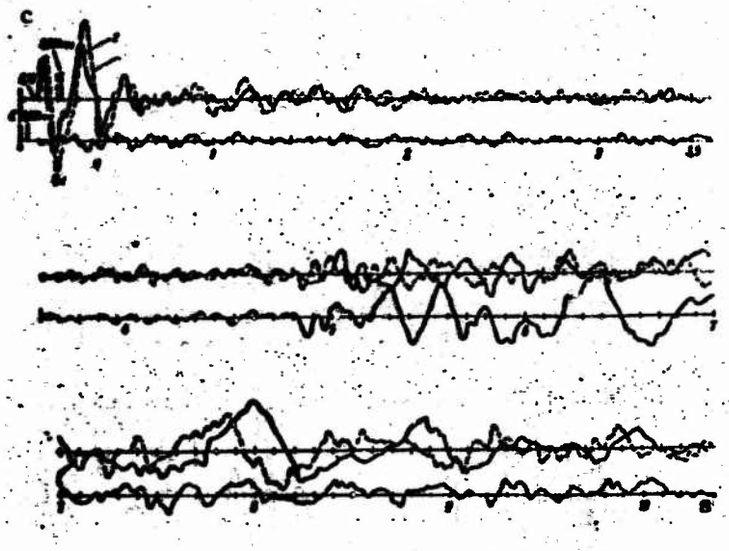

Fig. 10. Oscillograms of soil displacements at free surface on underground explosion of a 150-ton charge in granite. a) instruments mounted on a layer of soft soil several meters thick at a distance of 13 km from the epicenter; b) instruments installed on bedrock at a distance of 20 km from the epicenter; c) same, at a distance of 40 km.

surface is preferentially horizontal, and has practically the same amplitude at different depths near the surface. There is also a vertical motion component on the free surface [and] in its immediate vicinity. By way of example, Table 2 gives values of the maximum velocities and displacements in the compression wave at one of the points in the medium for the x (1x phase) and z-components at various instrument-placement depths h_p. A charge weighing 1 ton was exploded at a depth of 12m. The mass-velocity oscillograms for this point are given in Fig. 8.

While the motion has changed insignificantly at the first emergence at the x-component in the depth range covered, its amplitude in the vertical direction has dropped sharply even at the 6-meter depth.

After the positive and negative phases in the compression wave, which constitute practically the entire motion in an infinite massif, we sometimes observe multiphase oscillations caused by the compression wave near the free surface. Figure 9 shows x-component velocity

oscillograms at the 0- and 15-m depths. The motion is for all practical purposes limited to the positive and negative phases at the 15-meter depth, while tailing oscillations are evident on the free surface. We should note that the ground-vibration intensities measured at different registration points may differ even for the same explosion (Figs. 10 and 11).

According to the experimental data, the maximum velocity of soil motion in the longitudinal wave propagating along the free surface diminishes with distance in accordance with the same law as in the case of the unlimited massif, i.e., its decay can be expressed by Formula (1). It is important to stress two points in this context.

1. The free surface has practically no influence on the law of compression-wave attenuation. The fact that the damping of the compression wave does not increase as it propagates along the free surface means that even when the instrument is not buried particularly deep, the unloading from this surface arrives everywhere at the point of measurement at a time when the positive part of the compression wave has already practically ceased to act at this point, i.e., the unloading wave propagates at lower velocity than the compression wave.

The difference between the propagation velocities of the compression and decompression waves obviously results from natural fissuring and inhomogeneities of the rocks and, consequently, dissimilar elastic characteristics of the medium in compression and tension. Among other things, this is also indicated by the results of direct measurements of the tension and compression moduli of certain rocks (Table 3).

TABLE 3

Rock	$\frac{E_p}{E_c}$	$\frac{E_f}{E_c}$
Clay shales	0,3—0,9	0,3—0,5
Sandy shales	0,3—0,4	0,3
Sandstones	0,2—0,9	0,3—0,9

2. Propagation of the waves along the free surface has no substantial effect on the attenuation law. This means that in determining the nature of unknown waves propagating near the free surface, comparison of the attenuation laws of these waves is one of the basic criteria for determination of the divergence of the particular wave front.

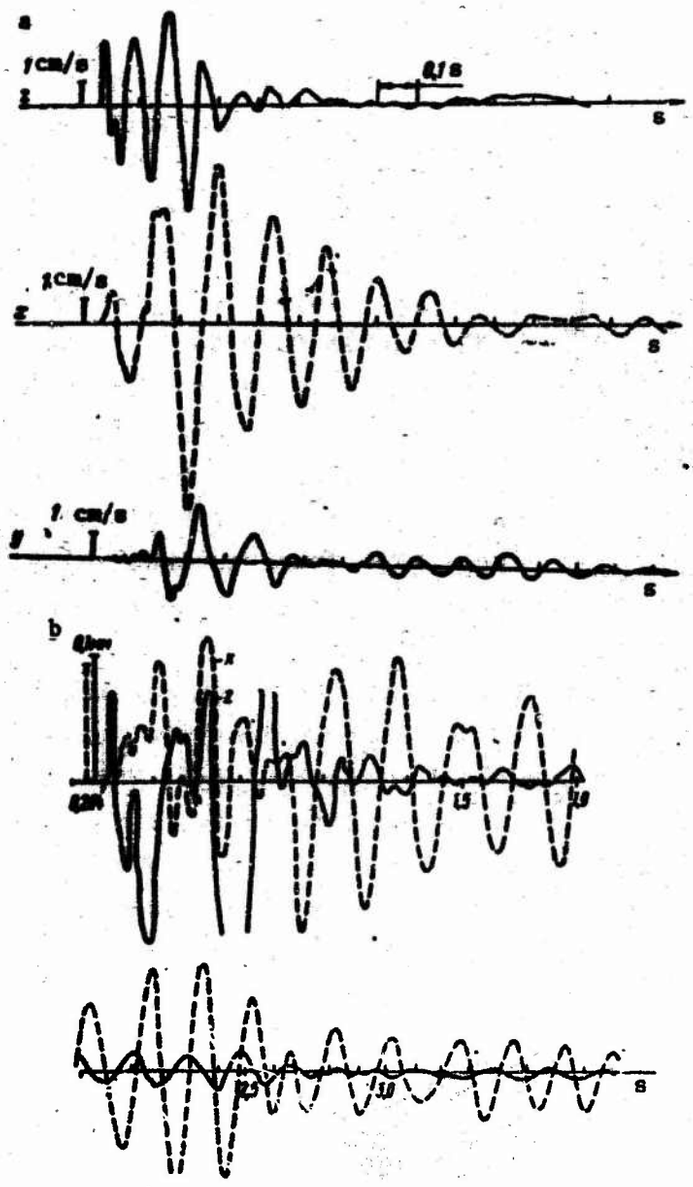

Fig. 11. Oscillograms of mass velocity (a) and displacement (b) of soil on free surface on explosion of a 10-ton charge buried 35 m deep in a rock massif with an overlying layer of soil. a) r = 0.6 km; b) r = 1.4 km.

The decompression wave is formed in the epicentral zone during the second stage of the blast (second source). Obviously, shaping of this wave begins at the time when the compression wave emerges at the free

surface at the blast epicenter. The time to form the decompression wave is determined by the time during which the soil in the epicentral zone heaves without losing its bond to the entire surrounding massif. During this time, the soil rising above the surface draws the contiguous zone of the medium along with it. Oscillogram placement of the times at which the decompression wave arrives at specific points is often made difficult by the fact that this arrival occurs against a background of soil motion following the compression wave. The most distinct phase of the decompression wave is the velocity- or soil-displacement maximum in the direction of the explosion. This maximum is marked 2x on the velocity oscillograms. After the soil has shifted toward the explosion, we observe a return motion. Phase 2x' on the oscillograms corresponds to the velocity maximum of the return motion. On the whole, the motion of the soil in the decompression wave is of low frequency by comparison with the motion in the longitudinal compression wave, and is oscillatory in nature. The initial motion of the soil toward the explosion and the subsequent return to the original position are strongest. Subsequent oscillations in the decompression wave are of comparatively short duration and small amplitude.

The propagation velocities of decompression waves near the free surface in real soils may be lower than the propagation velocity of the longitudinal compression waves. Table 1 lists velocity values for decompression waves in certain rocks as measured directly on oscillograms (the velocities of the 2x and 2x' phases). Direct decompression-wave velocity measurements showed that tensile strains propagate much slower in real rocks than do compressive strains. This difference is especially conspicuous in soils of the clay type and in other nonrocky soils.

According to the data of Table 1, the velocity of a decompression wave in clay is lower than that of the longitudinal compression wave by a factor of about 2. A consequence of this large velocity difference is that the decompression wave separates from the longitudinal compression wave even at comparatively short distances and is clearly manifest

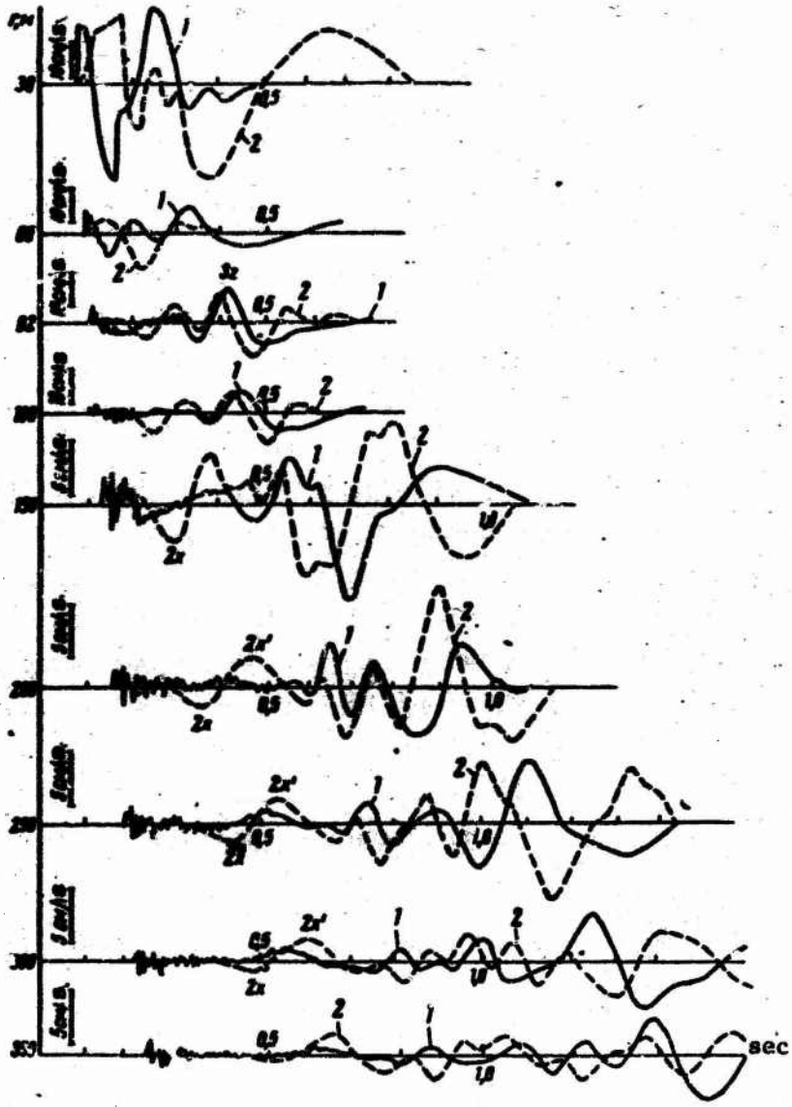

Fig. 12. Mass-velocity oscillograms on underground explosion of 1-ton charge at a depth of 4.5 m in clay.

as an independent wave. Figure 12 shows oscillograms of mass velocity in clay.

It is interesting to note that the velocity of the decompression wave varied with charge weight for explosions in clay (Table 4).

When charge weight was increased from 10^2 to 10^4 kg, the velocity increased steadily, but when the power of the explosion was increased

TABLE 4

Charge weight kg	Decompression wave velocity m/s	transverse compression wave velocity m/s
10^{2}	750	330
10^{3}	900	500
10^{4}	1250	700
10^{5}	1250	900

further, it remained constant.

In all probability, the dependence of decompression-wave propagation velocity in clay on charge weight is an accident that can be explained by inhomogeneity of the medium. The upper layers of the clays in which the experiments were conducted were weathered and characterized by lower transverse compression wave velocities. Since the smaller explosions were set off at correspondingly lesser depths, the decompression-wave velocities were also lower in these blasts. For explosions in rocky soils, no dependence of decompression-wave propagation velocity on charge weight was detected.

In most cases, the velocity of the decompression wave in real rocks is lower than that of the compression wave, because these rocks behave differently in compression and tension. This is explained, on the one hand, by the nature of the bonds between the individual rock particles, as, for example, in soft soils of the clay type. In such soils, a difference between the propagation velocities of shearing and tensile strains will in all probability be observed even in the presence of a perfectly homogeneous medium. On the other hand, the rocks may behave differently in compression and tension because of their natural fissuring, as, for example, in rocky soils. Cracks are almost always completely filled by water or sedimentary rocks; compressive strains are therefore transmitted well across these cracks. Transmission of tensile strains, on the other hand, is difficult, since there is no strong bond between particles.

Thus, the decompression-wave propagation velocity measured in an explosion is an elastic characteristic of a certain massif with consideration of the natural inhomogeneities that exist in it. Such a characteristic is more objective than analogous characteristics derived for individual specimens, since it pertains to a substantial volume of rock in the former case and considerable scatter of the quantities subject to determination is inevitable in the latter case, because of specimen inhomogeneity.

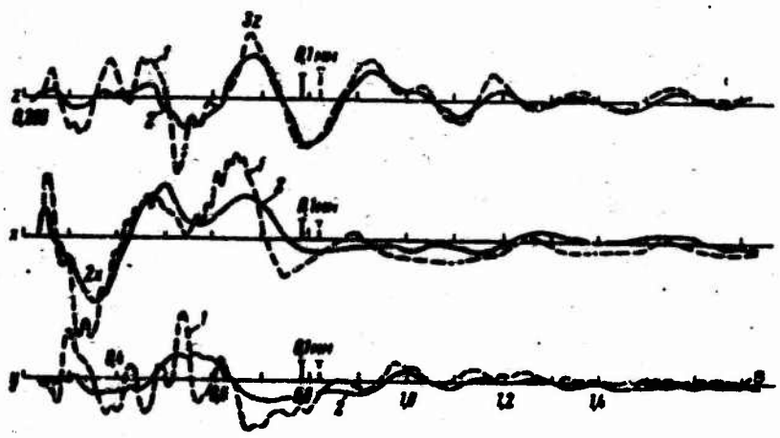

Fig. 13. Oscillograms of displacements of rocky soil during underground explosion. q = 150 tons; h_z = 75 m; r = 1500 m; 1) motion on free surface; 2) motion at depth of 110 m.

As we see from Fig. 8, the soil moves horizontally in the decompression wave near the free surface. Right at the surface, however, there is also a vertical component in the decompression wave, and it is nearly as large as the radial component. The vertical component decays quite rapidly with depth, while the motion in the horizontal direction undergoes practically no depthwise change. The absence of damping of the horizontal motion in depth indicates that this motion is not a surface motion, but involves a considerable part of the massif. On the other hand, the rapid damping of the vertical motion component with depth indicates that this motion is superficial. The appearance of the z-component of the motion is due, as in the case of the longitudinal compression wave, to the presence of the free surface. It is interesting to note the relation between wavelength and the thickness of the layer in which the surface motion is observed. Thus, the layer thickness is no more than 20 m for explosion of a 1-ton charge, while the decompression wave of this explosion is more than 300 m in length. This means that the influence of the free surface extends to a very limited depth that is much smaller than the wavelength. This statement also applies when the scale of the explosion is increased. Thus, on the explosion of a charge weighing 150 tons, there is practically no vertical component in the decompression wave at a depth of 110 m, while

the radial component undergoes almost no change (Fig. 13). Here the wavelength was over 1000 m, i.e., the influence of the free surface is manifest at comparatively shallow depths even in this explosion.

The maximum velocity of soil motion in the decompression wave decreases with distance in accordance with the law

$$u = A\left(\frac{\sqrt[3]{q}}{r}\right)^{1.7} \qquad (2)$$

The exponent in Formula (2) is the same for different soils and is practically equal in magnitude to the exponent in Formula (1). The similar laws of damping with distance for compression and decompression waves indicate that the decompression wave has a spherical front divergence and transfers energy uniformly in all directions. This is also indicated by the stable form of the soil motion in the decompression wave at various distances from the epicenter. It begins everywhere with displacement of the soil in the direction toward the explosion.

The coefficient A in Formula (2) is a constant that depends on soil type. Thus, it is 360 for rocky soil and 700 for clays. The differences in the coefficients A is obviously a consequence of the fact that different fractions of the energy are transmitted into the decompression wave in different soil types.

Our attention is drawn to the fact that the damping of compression and decompression waves in a given soil follows approximately the same law, although the lengths of these waves differ substantially (see Fig. 12). The existence of a consistent decay law for two waves of different lengths and the same divergence indicates that the absorption of energy from these waves with distance is approximately the same. The fact that no substantial increase in the attenuation of the shorter waves is observed when the wavelengths differ by a factor of about 3-5 is evidence of weak frequency-dependence of energy absorption. Even though this dependence does exist, the mechanism of energy dissipation associated with viscous friction forces is not decisive in this case. It appears that volume absorption of energy by dry friction between particles (Coulomb friction), which is proportional to stress and independent of time, is the most important factor.

The duration of the soil motion in the decompression wave toward the explosion is determined by the time during which the soil that heaves in the epicentral zone retains its bond to the surrounding massif. This means that the period of the ground oscillations in the decompression wave depends on the cohesiveness of the soil and its ability to withstand tensile strains without rupture. The dome shapes shown in Fig. 7 for various points in time indicate that the dome lift time without breakage is longest for explosions in soft soils of the clay type. Thus, on the explosion of a 1-ton charge in clay, the dome retains its bonds to the surrounding massif for 0.3-0.5 s, to judge from its surface. Accordingly, the oscillation period of a decompression wave in clay is longest, at about 0.25 s, by comparison with other soil types.

In rocky soil, detonation of charges of the same power as those used in the clay raises the ground in a dome for a very short time. The dome breaks and the central zone separates from the surrounding massif as soon as 0.04 s after the explosion. The rapid breakup of the dome signifies, firstly, rapid eruption of gaseous blast products, i.e., rapid unloading of the massif around the cavern, and, secondly, cessation of energy transfer into the surrounding massif from this most rapidly moving central part of the dome. Both of these factors tend to shorten the time during which the second source acts. The oscillation period in the decompression wave of an explosion in rocky soil is thus determined only by the duration of a certain initial stage of ground heave at the epicenter. For the explosion of the 1-ton charge in granite, the ground oscillation period in the decompression wave is about 0.08 s, i.e., shorter by a factor of about 3.5 than in clay.

Thus, the amount of blast-product energy used to radiate the decompression wave is smaller in an explosion in rocky soil than in an explosion in clay. On the basis of the above, we should expect the period and amplitude of the decompression wave to change as the setting depth of the charge is increased, since, on the one hand, later rupture of the dome becomes possible, and, on the other hand, the total expansion time of the blast products toward the free surface is shorter because of the greater weight of soil and its higher strength. Thus, the period of the oscillations is shorter by a factor of about 1.7, and the velocity of particle motion lower by a factor of 5-7 for a contact

explosion than for an explosion at a depth of $h_z/q^{1/3} = 1$ m/kg$^{1/3}$. If the soil layer above the charge is too thick, force equilibrium may intervene at comparatively small soil strains, i.e., there may be practically no heaving of the soil toward the free surface. Actually, experience has shown that the decompression-wave amplitude begins to decrease beyond a certain optimum depth.[4]

Increasing the power of the blast increases the volume of soil lifted in the central zone and lengthens the time during which the second source acts. As a result, the time during which energy is transferred from a certain central zone into the surrounding massif also increases, i.e., the vibration period of the soil in the radiated waves becomes longer. Soil-oscillation period depends as follows on charge weight:

for rocky soil

$$T = 6{,}5q^{1/6}, \quad \mu s \tag{3}$$

for clay

$$T = 60q^{0.21}, \quad \mu s \tag{4}$$

Formulas (3) and (4) are valid for charges weighing from 1 to 1000 tons. These formulas indicate that the oscillation period in rocky soil is shorter than it is in clay. The fact that the difference between the periods decreases with increasing blast power is extremely interesting. Thus, for the explosion of a 1-ton charge, the oscillation period in clay is about 3.5 times longer than in granite, while the difference is only a factor of 1.67 for charges weighing 1000 tons. As blast power is increased further, this difference will obviously become smaller. The equalization of the soil oscillation periods in the decompression wave with increasing blast power for explosions in the various media is a consequence of the increasing influence of gravity. Indeed, the influence of gravity in the heaving of the soil during the motion will increase with increasing charge weight, while the influence of the strength characteristics of the rock will decrease. More complete data on soil oscillation period as a function of charge weight are given in B.G. Rulev's paper.[5]

[4,5] See page 61 for footnotes.

Transverse S_z wave. The transverse S_z wave[6] is the wave formed together with the decompression wave during the second stage of an explosion near a free surface as a result of heaving of the soil in the epicentral zone. We should note that the fact that this wave exists is postulated on the basis of the motion characteristics of the medium in the central zone, which were described above and are cited in the paper by V.G. Lebedev et al. (see this collection). This assumption appears quite logical, since, like the bulk stresses, shearing stresses are also inevitable in a composite deformation of the medium. It is precisely these basic possible types of strains and, consequently, of waves that form the basis for deciphering of the wave pattern in an explosion. At the same time, a different approach is practiced in other quarters. Thus, for example, the oscillations that are associated with the S_z wave in the present paper are identified with the Rayleigh wave in the work of B.G. Rulev and other authors. In such treatment, the transverse wave is not detected at all, and, moreover, a wave whose excitation mechanism is unclear is introduced. This approach appears illogical. Such ambiguity of interpretation results from the fact that, as will be shown below, the S_z wave exhibits a number of surface-wave attributes.

The S_z wave appears on the vertical z- and radial x-components. Let us examine the properties of this wave. If we assume that the soil particles in the epicentral zone move along radii, i.e., if we represent the heaving of the ground as a displacement of certain conical surfaces relative to others, the transverse wave must have a conical divergence. Experience indicates, however, that the particles deviate from the radial direction toward the axis of symmetry in their motion. Hence the actual divergence of the transverse wave is intermediate between those of conical and cylindrical waves.

Thus, the shearing strains are originally excited in a certain upper layer with a depth approximately equal to the dimension of the heaving dome. The transverse wave obviously propagates through a certain layer near the free surface. The thickness of this layer may increase as the wave propagates. The transverse wave propagates at a lower velocity than the waves considered above, so that its appearance is registered later on the oscillograms (Fig. 13). On the oscillograms,

[6]See page 61 for footnote.

the individual phases of soil motion in the transverse wave are marked by the numeral 3 with the appropriate suffixes.

Transverse-wave velocities measured for certain soil types are given in Table 1. The ratio of transverse-wave velocity v_s to the velocity v_p of the longitudinal wave does not exceed 0.5 in any of the cases studied, and amounts to 0.25-0.3 in occasional cases.

Table 4 lists transverse-wave propagation velocities near the free surface for various scales of the explosion in clay. The velocity rise with increasing charge weight is due to the facts that the more powerful blasts were set off at appropriately greater depths and the medium was a gradient medium. A digression to determine how the wave parameters are influenced by the thickness of the upper layer, which, as a rule, is weaker than the basic soil, will therefore be appropriate.

It is customary to assume that if the layer thickness is much smaller than the wavelength, this layer need not be taken into account and the massif may be regarded as homogeneous. However, this interpretation is not quite correct. If the wave is excited and propagated in the basic massif, i.e., if a blast of sufficient power is detonated below the layer, this layer cannot in fact be left out of account in analyzing the motion of the basic massif. In this case, it acts as a comparatively light load resting on top of the basic massif. But the influence of the layer must be taken into account if the explosion took place directly in the layer. In this case, it is precisely in this layer that the transverse wave is first excited. The length of this wave is determined by the action time of the source in the layer and can, in principle, assume arbitrary values, including values substantially greater than the layer thickness. Since the wave originally propagates through the upper layer, it is the characteristics of this layer that determine the parameters of the transverse wave irrespective of the ratio of wavelength to layer thickness. For example, the velocity differences exhibited by the transverse wave in different explosions in clay result from precisely this phenomenon. The length of the wave observed on detonation of a 1-ton charge at a depth of about 5 m was more than 100 m, while the upper layer of weaker soil was no more than 10 m in depth. Explosions of 0.1-ton charges were set off at depths to 3.5 m, while 10-ton charges were buried at 9 m. The 1000-ton charge was detonated at a depth of 40 m in the basic clay massif. In

all of these explosions, the wavelength was far greater than the thickness of the upper layer, but the transverse wave still had different propagation velocities.

It is also necessary to note that the low transverse-wave velocities in the upper layer, despite its small thickness, can be traced to distances far exceeding the thickness of this layer. This is further evidence to the effect that the transverse wave propagates originally in an upper layer of small thickness and has a small divergence angle. Underlying layers, which are characterized by higher wave-propagation velocities, are slow to become involved in the motion. Consequently, these layers should be observed at comparatively longer distances in propagation of the transverse wave.

Unlike the S_z wave, the volume waves propagate in all directions, including downward from the source, from the very outset. As a result, the motion in the lower layers is excited much earlier and, consequently, at shorter distances. As the first preludes, we might expect the arrival of refracted or head longitudinal waves at the surface.

Since the S_z wave propagates in a certain layer along the free surface, the vertical component is the preferential component of soil motion in it. In the soil layer in which the transverse wave propagates, the amplitude on the z-component undergoes practically no change with depth. The oscillograms (see Figs. 8 and 13) indicate that for the explosions of the 1- and 150-ton charges, the maximum upward soil-motion amplitudes are practically the same at depths of 20 and 110 m, respectively, as on the free surface.

As in the case of the longitudinal and decompression waves, the interaction of the transverse wave with the free surface results in the appearance of a certain secondary motion in the surface layer. Along with the basic vertical direction, a radial (horizontal) component appears, with the two components nearly equal right at the free surface. The horizontal component damps out rapidly with depth, and at a depth much smaller than the wavelength, practically all that remains of the transverse wave is the vertical motion component. It is interesting to examine the trajectory of soil-particle motion in the transverse wave. Near the free surface, the trajectory takes the form of an ellipse along which the particles move counterclockwise (Fig. 14).

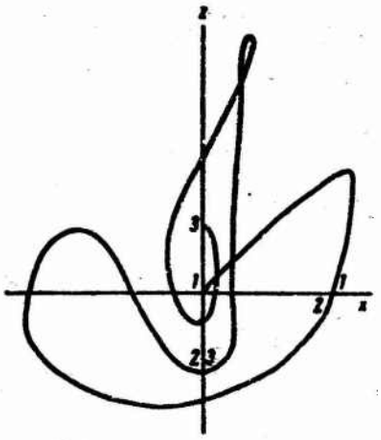

Fig. 14. Trajectory of soil-particle motion near the free surface at a distance of 245 m from the epicenter. q = 1 ton; h_z = = 12 m; 1-1) compression wave; 2-2) decompression wave; 3-3) transverse wave.

The low-frequency nature of the soil motion in the transverse S_z wave is reminiscent of the soil motion in the decompression wave. The parameters of the medium's motion vary smoothly in the transverse wave. The law of time variation of these parameters can be described in most cases by a trigonometric function of the sine or cosine type. The period of the soil oscillations in the transverse wave is always equal, at short distances from the charge, to the period of vibrations in the decompression wave, and this equality persists over a very broad range of variation of the absolute period values. Thus, for the explosion of a 1-ton charge in rocky soil, the period of the oscillations is about 0.07-0.08 s, while it exceeds 1 s for the explosion of a 1000-ton charge in clay. Despite the great difference in the blasting conditions (different rocks and charge weights), the relative equality of the periods in the transverse and decompression waves is always preserved. This confirms that these wave types have the same excitation source. All relationships that have been established for the oscillation period in the decompression wave, except for the variation of period with distance, are also fully applicable for the oscillation period in the transverse wave.

The soil vibration in the transverse wave is transitory in the zone close to the charge. The basic motion is exhausted, as in the case of the decompression wave, by the deflection of the points from their equilibrium position and their return to their original positions. The oscillations that follow are of low amplitude and comparatively short duration. If, however, a layer of soft soil covers the rock massif, the oscillations of the ground at the free surface or in the layer become quite substantial.

An interesting peculiarity of the transverse wave, as compared with the decompression wave, is that it propagates near the free surface in a certain layer whose thickness may increase as the wave moves away from the source. This property of the transverse wave proceeds from the mechanism by which it is excited. Data from the paper by B.G. Rulev and D.A. Kharin[7] can be cited as proof of the possibility of localization of transverse-wave energy in a certain layer. It is shown in this article that the distribution of the energy transferred by the transverse wave is determined basically by the nature of the source, i.e., having been excited in a certain elliptical zone, the transverse wave propagates for a long time with the minor axis of the ellipse as its preferential direction.

Propagation in a certain layer gives rise to a number of peculiarities inherent exclusively to transverse waves, as distinguished from waves with spherical divergence. One of these peculiarities is comparatively slow amplitude decay of the transverse wave with distance. If we represent the law of transverse-wave amplitude variation with distance in the form of a power monomial of the form

$$a \approx \frac{1}{r^n}, \tag{5}$$

the exponent n varies from 1 to 1.5, with no substantial difference being noted in the n for different soils. The range of variation of n is governed basically by the wide scattering of experimental values of the transverse-wave parameters. It will be recalled that n = 1.7-1.8 in the presence of spherical divergence of the wave front, i.e., it is larger than for a transverse wave.

The absolute values of the transverse-wave parameters depend on soil properties. Thus, for example, the maximum mass velocity in clay is approximately 2.5 times that in rocky soil. An even greater difference is observed in the maximum-displacement values.

An important property of the transverse wave, and one that is governed by its layerwise propagation, is the increase in the period of the soil oscillations in the wave with increasing distance. Thus, for explosion of a 150-ton charge, the oscillation period is 0.25 s at distances of 1-2 km and has increased to 1 s at a distance of about 40 km.

[7] See page 61 for footnote.

As in other waves, the increase in the transverse-wave oscillation period is obviously caused by the inhomogeneity of the upper layer.

Transverse S_y wave. Above, we examined the transverse S_z wave, which forms as a result of heaving of the ground in the epicentral zone in the presence of a horizontal free surface. The same kind of wave is also excited when the ground surface has slopes in the region of the epicenter. Here the nature of the S_z wave and its propagation laws remain about the same as for a horizontal free surface. However, an explosion near a free surface that is inclined at a certain angle to the horizontal has one peculiarity: when the ground heaves in the epicentral zone, the shearing-strain pattern will no longer have symmetry about the vertical axis. Together with the shears in the vertical direction, unsymmetrical shears also appear in the horizontal direction. The genesis of these shears might be traced in an explosion in soil inside the face of a vertical wall. In such an explosion, the shear strains near the charge will obviously have the same parameters as in an explosion near a horizontal surface, the only difference being that the strains will propagate in a vertical rather than in a horizontal layer, i.e., an explosion inside the face of a vertical wall will create a transverse wave that propagates in a vertical layer of the soil. It exhibits axial symmetry and a divergence intermediate between cylindrical and conical. Near the free surface, the intensity of the wave will not be the same in all directions from the blast epicenter: it will be highest in the direction that coincides with the plane of the vertical free wall and practically zero in the perpendicular direction, i.e., along the axis of symmetry. Such a transverse wave should be registered in the direction of maximum intensity by horizontal instruments whose axes point toward the explosion.

Thus, two transverse waves may be excited simultaneously in an explosion near an inclined free surface, with one, S_z, propagating in a horizontal layer, while the other, S_y, propagates in a vertical layer. The period of oscillation of the ground in the transverse S_y wave is equal, at short distances from the charge, to the oscillation period in the decompression wave and the S_t wave. Thus, for example, this period is the same for all three wave types at a distance of about 1.5 km from a 150-ton charge, equalling about 0.25 s. The difference between the periods confirms the common excitation source of all three waves.

Axial symmetry of the S_y wave may not always be strictly observed under real blasting conditions, since the shape of the free surface in the epicentral region is generally very complex. For an explosion under such conditions, there will be only the preferential propagation directions of the S_y wave along the free surface, those directions in which its intensity is highest. On the other hand, there may be no directions at all in which the transverse-wave amplitude is zero for explosions taking place under real conditions.

The intensity of motion in the S_y wave changes insignificantly with depth at a certain distance from the explosion. We see from the oscillograms (Fig. 13) that the amplitudes of the soil motion in the S_y wave are practically the same at the 110-m depth and at the free surface. Here it should be noted that the motion in the wave on the free surface is added to a comparatively high-frequency superficial vibration. Thus a true record of soil-motion amplitude on the free surface in the S_y wave can be obtained by averaging these surface vibrations.

The curious manner in which it propagates gives the transverse S_y wave certain properties that distinguish it from the S_z wave. Thus, for example, the propagation velocity of the transverse S_y wave increases more rapidly with increasing distance from the charge than does the velocity of the S_z wave. When a charge weighing 150 tons is detonated at a distance of up to 2 km, the velocities of the S_y and S_z waves are 2600 and 2400 m/s, respectively, i.e., closely similar. These figures pertain to velocity in the upper layers. At a distance of about 10 km, the velocity of the S_y wave is 3000 m/s, while that of $S_z \approx 2500$ m/s. This is because the motion in the S_y wave is transmitted very rapidly (at about the same rate as in a longitudinal wave with spherical divergence) into lower-lying, denser layers of earth, and a refracted wave, which has a higher apparent propagation velocity along the free surface than the transverse wave in the upper layers, makes its appearance at comparatively short distances from the charge. As a result, the appearance of the S_y wave on the oscillograms always occurs somewhat earlier than that of the S_z wave, even though they are of the same nature.

As in the S_z wave, the average period of the vibrations increases with distance in the transverse S_y wave.

RAYLEIGH AND LOVE WAVES

The wave patterns observed in explosions can be accounted for by the action of longitudinal and transverse waves alone, without taking Rayleigh and Love surface waves into consideration, although waves that exhibit the principal attributes of these surface waves (for example, S_z and S_y) stand out quite clearly on oscillograms. In deciphering blast oscillograms, most investigators take the ground vibrations that are caused, in our opinion, by the transverse S_z wave as a Rayleigh wave, and the oscillations in the S_y wave as a Love wave. The reason for this treatment is the fact that, by virtue of the specific peculiarities of their excitation, the transverse S_z and S_y waves have certain attributes that formally justify classifying them as surface-type waves. In essence, however, the transverse S_z wave has nothing in common with the Rayleigh surface wave, nor the transverse S_y wave with the Love wave. To demonstrate more clearly the incorrectness of such identification, let us consider the possibility of formation of a Rayleigh surface wave.

As we know, the possibility was first suggested by Rayleigh in 1887 on the basis of theoretical solution of the problem of steady-state, stationary vibration of an elastic half-space. Analyzing these oscillations, Rayleigh found that a certain motion of superficial nature is observed near the free surface and is governed by the presence of the surface, which is free of normal stresses. He indicated certain attributes of this motion and, by analogy with surface waves in water, advanced the hypothesis that surface-type waves near the surface of the ground might be possible.

Oscillations that have a number of the attributes indicated by Rayleigh have indeed been detected in deciphering earthquake and blast seismograms. They were called Rayleigh surface waves. However, there is not at the present time any clear notion as to the mechanism by which Rayleigh surface waves form when vibrations are excited by such a nonstationary source as an explosion.

As we noted above, the data of the present study indicated that the vibrations taken for Rayleigh waves may be of a totally different nature. The same data permit analysis of the free-surface effect and hence evaluation of the possibility of formation of Rayleigh surface waves.

It was shown with reference to three basic wave types that, in full agreement with theory, the presence of a free surface results in the appearance of a certain surface motion with features of the motion investigated by Rayleigh. Thus, for example, this motion decays rapidly with depth. The particle trajectory near the surface in each wave is nearly elliptical in shape, and in the transverse S_z wave the particles even move counterclockwise (see Fig. 14). All of these facts indicate that the surface motion observed is analogous to that examined by Rayleigh. It is precisely this motion that may be the source of Rayleigh surface waves. But since it is observed in the passage of all the waves, each of them may be a source of Rayleigh surface wave excitation.

Thus, the Rayleigh surface wave may be represented as a certain inertial motion that will persist in the surface layer after passage of a certain volume wave and will then be transmitted in this layer from some particles to others in the form of an independent wave. Since the surface motion is excited at every point on the free surface, each point may be a source that radiates a surface wave. Hence it follows that the motion at a certain point should continue long after each wave owing to the arrival of surface waves from preceding points at this point. However, this phenomenon is not observed in the experiments. If bedrock crops out onto the free surface and the recording instruments are mounted on the basic massif, there is practically no motion of the ground after passage of the waves. The vibrations of the surface layer also vanish almost immediately after culmination of the motion in the main wave, which is the exciter of the free-surface vibrations.

If we consider the relatively small thickness of the layer in which the surface motion is excited, i.e., the small stored energy of this motion, we can readily appreciate how rapidly it will be dissipated.

Comparatively intense and protracted inertial vibrations of the ground are observed when the upper layers are broken and poorly bonded to the base massif. The most favorable case for excitation of these vibrations near the free surface is that of a layer of soft soil overlying a rock base. In this case, rather prolonged vibration of the upper layer is generally observed after passage of each wave, and

independent waves may form in the layer. The long persistence of the vibrations in the upper layer is due to the fact that the energy of these vibrations is "locked" into the layer and is absorbed in a limited volume of soil.

Let us consider the question of the Love surface wave.

In some earthquakes, intense low-frequency vibrations are also observed on the third azimuthal component of the motion in addition to the vibration of the ground in the vertical z and radial r directions. These vibrations have the attributes of an independent wave and have come to be known as the Love wave. The propagation velocity of the Love wave approaches that of the transverse waves [1]. In our opinion, identification of the vibrations observed on the azimuthal component with the Love surface wave is incorrect, and for the following reasons.

As a rule, vibration of the ground on the azimuthal component is observed everywhere in experiments, including in the immediate vicinity of the charge. Thus, for example, on explosion of the 150-ton charge, motion of the ground on the third component in the form of an independent wave was observed even at distances of a few hundred meters and beyond. But on the basis of the inherent interference nature of the Love wave, the formation of this wave would be expected at distances of more than ten kilometers. The existence of motion on the y-component in the immediate vicinity of the source is evidence that the wave generating it is not an interference wave. Moreover, since the low-frequency aspects of the ground vibrations on the y- and z-components are the same, it is quite obvious that the transverse S_z wave and the wave that appears on the y-component must have the same source.

The transverse S_y wave is the most realistic cause of excitation of the azimuthal-component vibrations. The low-frequency nature of these vibrations is explained by the motion of the ground at the source itself, and not as a result of interference phenomena, as is assumed in the Love wave. If we relate the y-component ground motion to the Love wave, it will then be necessary to demonstrate the possibility of formation of a plane transverse wave in the explosion. According to Love's theory, it is precisely this wave that may lead to formation of a surface wave with particle motion in the horizontal plane. But, as we know, an explosion is a concentrated source, and plane transverse waves cannot be excited by such a source.

The phenomena that Love investigated theoretically are possible during propagation of the transverse S_y wave.

* * *

It has been established as a result of the studies made that an explosion near a free surface is a complex wave source and cannot be described simply in the form of a center of expansion that radiates only a longitudinal compression wave. The elastic-stress field that arises around a spherical cavern and in the case of a camouflet explosion and offsets the cavern gas pressure after radiation of the wave may be a secondary radiation source in an explosion near a free surface. With the rapid pressure drop that takes place in the gaseous blast products as a result of cavern expansion toward the free surface, and under the influence of the free surface itself, the stress field around the cavern is relieved quite rapidly. The energy of the elastic stresses in the medium and that of the gaseous blast products cause the medium to heave up into a dome in the epicentral zone. Volume and shear strains are developed as a result of this heaving, which takes place much more slowly than the compression-wave-radiating process. The volume strains are tensile in nature and give rise to a wave of tensile stresses (decompression wave). The shearing strains that arise when the dome-shaped elevation of the medium appears exhibit axial symmetry and are capable of radiating a transverse wave whose front has a cylindrical divergence, with the result that the transverse wave decays much more slowly with distance from the charge than does the longitudinal wave.

Thus, an explosion near a free surface is capable of radiating at least three independent waves: a longitudinal compression wave in the first stage and longitudinal and transverse waves in the second. The latter are waves of comparatively long period because of the slower development of the explosion in this stage. All three wave types explain the basic features of the wave pattern observed in explosions detonated under various conditions. Identification of the corresponding segments of the long-period vibrations on oscillograms with the transverse wave is most questionable. Without justification, many investigators regard these vibrations as due to the action of a Rayleigh surface wave. In a zone with a radius of several tens of kilometers, surface waves make no

appreciable contribution to the general wave pattern during explosions of charges ranging from 1 ton to 1000 tons in weight. In all probability, their influence may make itself felt at much greater distances.

References

1. Savarenskiy, Ye.F. and D.P. Kirnos, Elementy seysmologii i seysmometrii (Elements of seismology and seismometry). Gosudarstvennoye izd-vo tekhniko-teoreticheskoy literatury, 1955.

2. Kuz'mina, N.V., A. N. Romashov, B. G. Rulev, D. A. Kharin and Ye.I. Shemyakin. "Seysmicheskiy effekt vzryvov na vybros v neskol'kikh svyaznykh gruntakh" (Seismic effect of excavating blasts in several cohesive soils). Trudy IFZ (Transactions of the Institute of Earth Physics), No. 21/188. Izd-vo AN SSSR, 1962.

3. Rulev, B.G. Podobiye voln szhatiya pri vzryvakh v gruntakh (Similarity ofcompression waves in underground explosions). PMTF, 1963, No. 3.

4. Rulev, B.G. Energiya v poverkhnostnoy volne Releya pri vzryvakh v razlichnykh gornykh porodakh (Energy in the Rayleigh surface wave in explosions in various types of rocks). "Izv. AN SSSR, seriya fizika Zemli", 1965, No. 4.

5. Dokuchayev, M.M., V.N. Rodionov, and A.N. Romashov. Vzryv na vybros (The excavating explosion). Izd-vo AN SSSR, 1963.

6. Khristoforov, B.D. and A.N. Romashov. Opredeleniye parametrov volny szhatiya v skal'nom grunte po rezul'tatam izmereniya davleniya v skvazhinakh s vodoy (Determination of compression-wave parameters in rocky soil from results of pressure measurement in water wells). "Fizika goreniya i vzryva", 1967, No. 3.

7. Kol'skiy, G. Volny napryazheniy v tverdykh telakh (Stress waves in solids). Izd-vo "Inostrannaya literatura", 1955.

8. Tsvetkov, V.M. O vzryve v peschanom grunte (The explosion in sandy soil). PMTF, 1962, No. 5.

Footnotes

Manuscript page	
24	[1]See paper by V.B. Lebedev et al. in this collection.
25	[2]See paper by B.G. Rulev in this collection.
33	[3]See footnote to page 25.
48	[4]See footnote to page 25.
48	[5]See this collection.
49	[6]A plane transverse wave with similar motion is denoted by SV in seismology. A different symbol is used in this article because the wave under consideration is not a strictly plane wave.
53	[7]See this collection.

REVERSE BLANK

Symbol list

Manuscript page	Symbol		English equivalent
32	з	z	charge
38	п	р	instrument

REVERSE BLANK

UNCLASSIFIED

Security Classification

DOCUMENT CONTROL DATA - R & D

(Security classification of title, body of abstract and indexing annotation must be entered when the overall report is classified)

1. ORIGINATING ACTIVITY (Corporate author)
Foreign Technology Division
Air Force Systems Command
U. S. Air Force

2a. REPORT SECURITY CLASSIFICATION
UNCLASSIFIED

2b. GROUP

3. REPORT TITLE
AN INVESTIGATION OF CAVERN DEVELOPMENT IN THE CAMOUFLET EXPLOSION

4. DESCRIPTIVE NOTES (Type of report and inclusive dates)
Translation

5. AUTHOR(S) (First name, middle initial, last name)
Rodionov, V. N. , Sizov, I. A. , and Tsvetkov, V. M.

6. REPORT DATE
1968

7a. TOTAL NO. OF PAGES
23

7b. NO. OF REFS

8a. CONTRACT OR GRANT NO.
F33657-70-D-0607-P002

b. PROJECT NO. 72301-74

c.

d. DIA Task No. T69-01-23

9a. ORIGINATOR'S REPORT NUMBER(S)
FTD-HC-23-87-70

9b. OTHER REPORT NO(S) (Any other numbers that may be assigned this report)

10. DISTRIBUTION STATEMENT
Distribution of this document is unlimited. It may be released to the Clearinghouse, Department of Commerce, for sale to the general public.

11. SUPPLEMENTARY NOTES

12. SPONSORING MILITARY ACTIVITY
Foreign Technology Division
Wright-Patterson AFB, Ohio

13. ABSTRACT

The formation of cavities in rock is closely related to the processes of explosion development, but the volume of cavities is strongly dependent on the strength of the material. For weak clays and loams, the ratio of cavity volume to weight of charge is 10 (superscript 2) minus 10 (superscript 3) liters/kg of TNT, whereas for strong rocks this ratio is but a few liters per kilogram of TNT. The effect of a concentrated charge is studied for a charge depth sufficient to prevent shattering of rock at the surface. Starting with equations for stresses and strains in the medium, the authors derive a given expression to define the maximal volume of cavities. To determine the maximum volume of cavities, it is necessary to know the cavity velocity or the kinetic energy of the medium at some initial moment. It is most suitable to select initial parameters for the instant when the compressional wave converts the medium to the plastic state, that is, when the plasticity front begins to lag behind the front of the compressional wave. Computations agree well with experimental data. Orig. art. has: 5 figures, 3 tables, and 29 formulas. [AT8032891]

DD FORM 1 NOV 65 1473

UNCLASSIFIED

Security Classification

14 KEY WORDS	LINK A		LINK B		LINK C	
	ROLE	WT	ROLE	WT	ROLE	WT
Rock						
Material Crushing						
Underground Explosion						
Clay						

UNCLASSIFIED
Security Classification

DOCUMENT CONTROL DATA - R & D

(Security classification of title, body of abstract and indexing annotation must be entered when the overall report is classified)

1. ORIGINATING ACTIVITY (Corporate author)
Foreign Technology Division
Air Force Systems Command
U. S. Air Force

2a. REPORT SECURITY CLASSIFICATION
UNCLASSIFIED

2b. GROUP

3. REPORT TITLE
ON THE NATURE OF CERTAIN GROUND WAVES EXCITED BY AN UNDERGROUND EXPLOSION

4. DESCRIPTIVE NOTES (Type of report and inclusive dates)
Translation

5. AUTHOR(S) (First name, middle initial, last name)
Romashov, A. N.

6. REPORT DATE	7a. TOTAL NO. OF PAGES	7b. NO. OF REFS
1968	39	8

8a. CONTRACT OR GRANT NO.	9a. ORIGINATOR'S REPORT NUMBER(S)
F33657-70-D-0607-P002	
b. PROJECT NO. 72301-74	FTD-HC-23-87-70
c.	9b. OTHER REPORT NO(S) (Any other numbers that may be assigned this report)
d. DIA Task No. T69-01-23	

10. DISTRIBUTION STATEMENT
Distribution of this document is unlimited. It may be released to the Clearinghouse, Department of Commerce, for sale to the general public.

11. SUPPLEMENTARY NOTES	12. SPONSORING MILITARY ACTIVITY
	Foreign Technology Division Wright-Patterson AFB, Ohio

13. ABSTRACT

It is shown that a near-surface explosion is a complex source of waves and cannot be considered merely a center of expansion, emitting a single longitudinal compressional wave. This complex motion of surface particles is illustrated. The field of elastic stresses arising around the spherical cavity of an underground explosion tends to equalize the gas pressure after emission of the wave, whereas in a near-surface explosion, the stresses may be a secondary source of emission. When the gas pressure declines rapidly among the gaseous products produced by expansion of the cavity toward the free surface (and because of the free surface itself), the stress field around the cavity is rapidly reduced. Energy of the elastic stresses in the medium and energy of the gaseous products of the explosion cause a dome-like uplift of the material above the shot site, and volume and shear strains develop. Volumetric strains are tensional, giving rise to tensional (rarefaction) waves. Shear strains have axial symmetry and generate transverse waves with a front that is approximately cylindrical, attenuating with distance more slowly than the longitudinal waves. Near-surface explosions may thus generate at lease three independent waves: compressional during the first stage, longitudinal and transverse during the second. Orig. art. has: 14 figures, 4 tables, and 5 formulas. [AT8032898]

DD FORM 1 NOV 1473

UNCLASSIFIED
Security Classification

14. KEY WORDS	LINK A		LINK B		LINK C	
	ROLE	WT	ROLE	WT	ROLE	WT
Underground Explosion Elastic Wave Stress Distribution Transverse Wave Rarefaction Wave						